Journal of Structural Geology 32 (2010) 1557–1575

Contents lists available at ScienceDirect

Journal of Structural Geology

journal homepage: www.elsevier.com/locate/jsg

Review Article

A review of recent developments concerning the structure, mechanics and fluid flow properties of fault zones

D.R. Faulkner[a,*], C.A.L. Jackson[b], R.J. Lunn[c], R.W. Schlische[d], Z.K. Shipton[e], C.A.J. Wibberley[f], M.O. Withjack[d]

[a] Department of Earth and Ocean Sciences, University of Liverpool, Liverpool, UK
[b] Department of Earth Science and Engineering, Imperial College London, UK
[c] Department of Civil Engineering, University of Strathclyde, Glasgow, UK
[d] Department of Earth and Planetary Sciences, Rutgers University, Piscataway, New Jersey, USA
[e] Department of Geographical and Earth Sciences, University of Glasgow, Glasgow, UK
[f] Total France EP, CSTJF, Av. Larribau, Pau, France

ARTICLE INFO

Article history:
Received 11 December 2009
Received in revised form
1 June 2010
Accepted 16 June 2010
Available online 11 August 2010

Keywords:
Faults
Structure
Fluid flow
Mechanics
Earthquakes

ABSTRACT

Fault zones and fault systems have a key role in the development of the Earth's crust. They control the mechanics and fluid flow properties of the crust, and the architecture of sedimentary deposits in basins. We review key advances in the study of the structure, mechanics and fluid flow properties of fault zones and fault systems. We emphasize that these three aspects of faults are intimately related and cannot be considered in isolation. For brevity, the review is concentrates on advances made primarily in the past 10 years, and also to fault zones in the brittle continental crust. Finally the paper outlines some key areas for future research in this field.

1. Introduction

Fault zones control a wide range of crustal processes. Although fault zones occupy only a small volume of the crust, they have a controlling influence on the crust's mechanical and fluid flow properties. Much recent work has concentrated on describing and understanding the importance of the structure, mechanics and fluid flow properties of fault zones. This has involved field observations, laboratory experiments, seismology, hydrogeology, and analytical and numerical modelling.

Brittle fault zones are lithologically heterogeneous, anisotropic and discontinuous. Faults are complex zones composed of linked fault segments, one or more high strain slip surfaces nested within regions of high and low strain (often called fault core and damage zone), Riedel shears, splay faults, dilational and contractional jogs, and relay ramps (Rawling et al., 2001; Shipton and Cowie, 2001; Faulkner et al., 2003; Childs et al., 2009). Individual fault zones commonly show significant variation in complexity along strike or down dip, even over relatively short distances (Schulz and Evans, 2000; Shipton and Cowie, 2001; Kirkpatrick et al., 2008; Lunn et al., 2008). Fault zone structure, mechanics and permeability can vary strongly both over geological time (e.g. Eichhubl et al., 2009) and at timescales relevant to a variety of industrial applications.

The strength of the lithosphere varies with depth, temperature and mineralogy (Kohlstedt et al., 1995) but a major load-bearing region is likely present at the base of the seismogenic zone at $\sim$15 to 20 km depth for normal continental crust. The mechanical properties of faults at this depth are thus inferred to control to some extent the strength of the entire crust. This inference is supported by observations of crustal stress magnitudes at shallower crustal levels that appear to be limited by the typical frictional strength of faults (Townend and Zoback, 2000). A related goal to characterizing the mechanical properties of faults at depth is to understand the earthquake process from nucleation and propagation to arrest.

Faults play an important role in controlling the migration of crustal fluids. One example of this is hydrocarbon migration, accumulation and leakage in sedimentary basins. At the basin scale,

* Corresponding author.
E-mail address: faulkner@liv.ac.uk (D.R. Faulkner).

0191-8141/$ – see front matter © 2010 Published by Elsevier Ltd.
doi:10.1016/j.jsg.2010.06.009

faults and fault-related folds control subsidence patterns and hence the distribution of thermally mature zones (e.g. Brister et al., 2002). Faults are also a key component of many hydrocarbon plays; they also may control discrete subsurface pressure cells (e.g. Grauls et al., 2002). At a smaller scale, a better understanding of the role of faults in compartmentalizing fields will yield better estimates of hydrocarbon production (e.g. Manzocchi et al., 1999). Increasingly, the recognition of high transient permeability along faults induced by hydrocarbon production (Losh and Haney, 2006) has focussed interest on the temporal variation of fault-zone permeability. Ore deposits are also commonly related to fault zones due to episodic, localized hydrothermal flows that occur during and immediately after periods of fault movement (e.g. Cox et al., 2001; Sibson, 2001).

Characterizing the fluid flow properties of the crust is necessary to facilitate the development of deep-waste storage repositories (e.g. Ferrill et al., 1999; Douglas et al., 2000), to allow sequestration of industrially-produced greenhouse gases (Streit and Hillis, 2004; Dockrill and Shipton, 2010) and to realize the potential of geothermal energy in appropriate locations (Rowland and Sibson, 2004; Fairley, 2009). The physical characteristics and properties of faults will play an important role in regional crustal fluid flow that might affect such applications.

This paper concentrates on three primary aspects of fault zones and fault systems; their structure, mechanics and fluid flow properties. We emphasize that these three aspects are inextricably coupled and this is highlighted in Fig. 1. Much recent research reflects efforts to understand the nature and processes behind this coupling. For instance, fault rocks are commonly altered (Evans and Chester, 1995) and are not simply a granulated product of their protolith. In fact, in the upper crust, many fault rocks may be viewed as low- to medium-grade metamorphic rocks, with authigenic growth of clays and other minerals. A close-knit coupling exists between deformation, mechanics and fluid flow in fault zones by deformation- and reaction-driven changes in porosity and permeability, and fluids causing changes in deformation mechanisms through fluid-rock interactions in fault zones (e.g. Rutter and Brodie, 1995; Wibberley and McCaig, 2000; Eichhubl et al., 2005; Holyoke and Tullis, 2006; O'Hara, 2007). The impact on fault rheology, such as by fluid-enhanced reaction softening, may be considerable (Imber et al., 2001; Gueydan et al., 2003; Jefferies et al., 2006a).

Given the importance of fault zones and fault systems, a vast body of work covers their development and properties. In this paper we review important classical concepts but concentrate on key advances in our understanding of fault zones over the past ~10 years. Further, we limit our discussion to upper crustal faults developed in the continental crust (i.e. those in the top 20 km of the crust). The review is perhaps biased towards the interests of the authors and concentrates on what we see as important issues reading fault zones. A number of excellent review articles have been published that refer to earlier work and the reader will be directed to these for not only a more historical view on the development of studies in this field, but more detail regarding the different disciplines involved.

This review concentrates first on the structure of fault zones and fault systems, including scaling relationships that can help in deciphering how fault zones develop and grow. Second, we discuss the mechanics of fault zones; this involves topics ranging from laboratory experimentation to modelling of earthquake rupture. Last, we address the topic of fluid-flow properties of faults, involving studies from *in situ* observations of fluid flow, laboratory experiments and modelling. We conclude by highlighting some key outstanding questions.

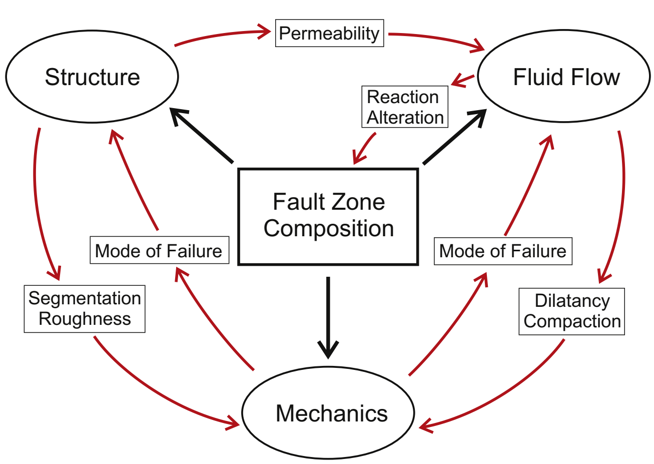

Fig. 1. Flow diagram showing inter-relationships among the three main topics of structure, mechanics and fluid flow. Mode of failure refers to whether or not seismic slip occurs.

2. Structure and development of fault zones and fault systems

2.1. Typical fault zone structure

A simple conceptual model for fault zone structure, developed over the past 20 years, involves strain that is localized in a fault core surrounded by a distributed zone of fractures and faulting in the damage zone (Fig. 2, see references in Wibberley et al., 2008). The fault core generally consists of gouge, cataclasite or ultracataclasite (or a combination of these), and the damage zone generally consists of fractures over a wide range of length scales and subsidiary faults. Strain may be homogeneously distributed across the fault core (Rutter et al., 1986; Faulkner et al., 2003) or may be highly localized onto discrete slip surfaces (Chester and Logan, 1986; De Paola et al., 2008). Brittle fault rocks have previously been considered chaotic, but detailed observations show that they are highly structured, commonly containing P foliations, Riedel shears and Y shears (Logan et al., 1979; Chester et al., 1985; Rutter et al., 1986; Jefferies et al., 2006b). Additionally, fault breccias, such as those described by Caine et al. (2010) can occur as part of the fault core in areas where movement involving fault jogs results in dilatation.

Recent research has questioned the general applicability of this simple model. Fault zones may contain a single fault core (sometimes with branching subsidiary faults), or the fault core may branch, anastomose and link, entraining blocks or lenses of fractured protolith between the layers (Fig. 2b; Faulkner et al., 2003). A comparison between the Punchbowl fault (Chester et al., 1993) and the Carboneras fault (Faulkner et al., 2003), two 40 km-displacement strike-slip faults that operated at similar depths, illustrates the effect of the contrast in mechanical properties between fault zone and protolith. The widths of the core zones of these faults (50 cm for the Punchbowl fault in granite and low-porosity sandstones versus multiple strands over a 1 km wide zone for the Carboneras fault in predominantly mica schists) may reflect differences in the mechanical strength contrast between protolith and the deformation zone. The second style of fault zone structure has been observed in the SAFOD borehole, where multiple fault strands, individually up to several metres thick, exist and at least two of these strands of fault gouge are moving simultaneously (Zoback et al., 2010). The schematic diagrams in Fig. 2 purposely have no scale to illustrate that these fault zone structures occur at a variety of scales. The internal structure of fault zones might provide a useful indication of their mechanical properties (Faulkner and Rutter, 2003; Biegel and Sammis, 2004; Faulkner et al., 2008).

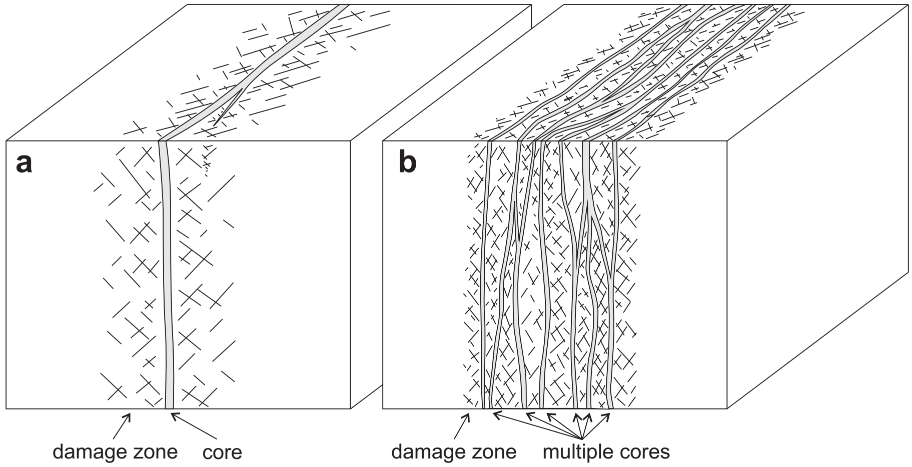

Fig. 2. Typical fault zone structures. (a) Shows a single high-strain core surrounded by a fractured damage zone (after Chester and Logan, 1986) and (b) shows multiple cores model, where many strands of high-strain material enclose lenses of fractured protolith (after Faulkner et al., 2003).

Localization may be further enhanced where a fault juxtaposes two protoliths of highly contrasting competence, such as the Median Tectonic Line, Japan (e.g. Wibberley and Shimamoto, 2003).

Fault zone structure depends on the depth of formation (e.g. Ishii et al., in press), protolith, tectonic environment (e.g. strike-slip, extension or compressional), magnitude of displacement and fluid flow. For instance, faults in low porosity rocks (Balsamo et al., 2010) generally have a fine-grained fault core surrounded by a fracture-dominated damage zone. In contrast, coarser grained, high porosity rocks commonly develop by the formation and amalgamation of low porosity deformation bands followed by the nucleation and propagation of high permeability slip surfaces (Fossen et al., 2007).

Several authors provide qualitative descriptions of fracture damage zones surrounding a fault core (e.g. McGrath and Davison, 1995; Shipton and Cowie, 2003; Kim et al., 2004; Berg and Skar, 2005; Cembrano et al., 2005; Johansen et al., 2005; Cook et al., 2006; de Joussineau and Aydin, 2007; Fossen et al., 2007). Damage zones contain fractures at a range of different scales from grain-scale microfractures to macrofractures that may accommodate small shear offsets and a small quantity of cataclasite. It can be difficult to distinguish between subsidiary fault structures (which may be viewed as faults in their own right) and fault damage zone fractures. In the tip zones of large displacement faults in particular the complexity of deformation is marked (Kirkpatrick et al., 2008). The orientation of the macroscopic deformation surrounding fault tips may include horsetail geometries, wing cracks and synthetic or antithetic subsidiary faults (e.g. de Joussineau and Aydin, 2007; Moir et al., 2010). In low porosity rocks or under low effective stress conditions, damage zones consist of dilatant fractures (Blenkinsop, 2008), whereas higher porosity rocks often develop structures in their damage zones such as compaction bands in sandstone (analogous to anticracks) or cataclastic deformation bands (e.g. Johansen et al., 2005; Fossen et al., 2007).

Quantitative studies of damage zones, commonly involve determining the density of fractures (usually from line counting) as a function of distance from the fault core. For low porosity rocks, macrofractures (mesoscale features that may be readily identified in the field) and microfractures (measured from orientated thin-sections) commonly show an exponential decrease with distance from the fault core (Vermilye and Scholz, 1998; Wilson et al., 2003; Mitchell and Faulkner, 2009) (Fig. 3). This relationship has been linked to the decay of stress away from a fault tip predicted from fracture mechanics models. Microfractures in deformation band-dominated damage zones in high porosity sandstones show no observable change of microfracture density surrounding faults (Anders and Wiltschko, 1994; Shipton and Cowie, 2001) due to the different micromechanics of deformation-band faulting and

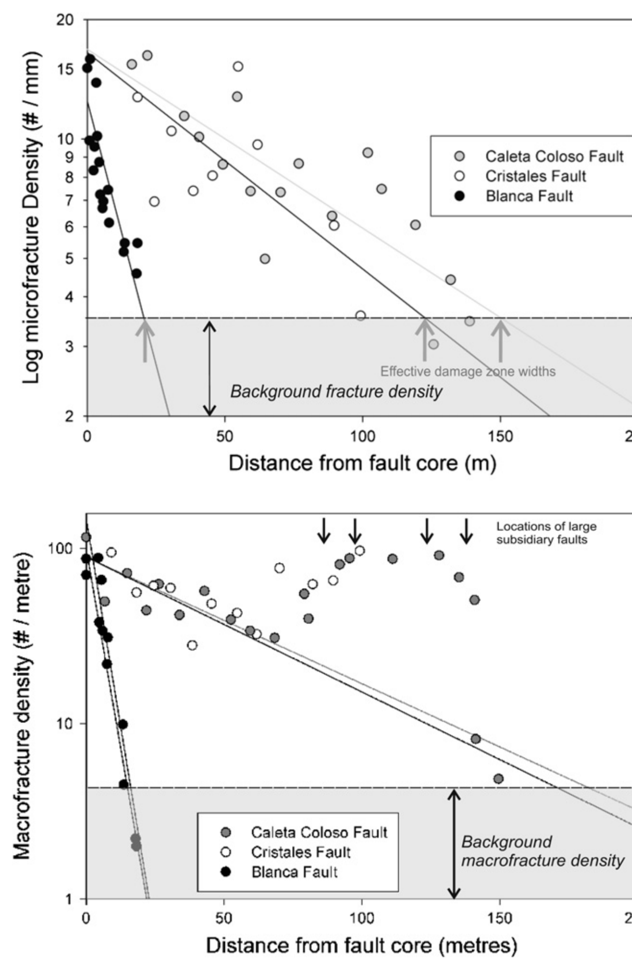

Fig. 3. An example of (a) microfracturing and (b) macrofracturing surrounding three strike-slip fault zones in northern Chile. The fault zones are in low porosity crystalline rocks and the Caleta Coloso fault has ∼5 km of displacement, the Cristales fault has 220 m of displacement and the Blanca fault 35 m of displacement. From Mitchell and Faulkner (2009).

fracture-dominated faulting (see Fig. 4). Nevertheless, where damage zones are dominated by deformation bands, these may show an exponentially decreasing density from faults in high-porosity sandstone (Berg and Skar, 2005; de Joussineau and Aydin, 2007), although in at least some cases, fault localization occurs once the damage zone has already developed (Saillet and Wibberley, 2010).

A maximum microfracture density is often attained immediately adjacent to the fault core that is dependent on rock type but independent of the fault displacement (Fig. 3). Although only three faults are shown in Fig. 3, three additional faults with smaller displacements (of 13 cm to 2 m) showed a similar maximum fracture density (of ~20 per mm) (Mitchell and Faulkner, 2009). This is suggestive of a critical amount of fracture damage that the rock can accumulate at the boundary between the fault core and the damage zone. The same type of fracture damage distribution occurs at the small scale (i.e. mm) in experiments (Janssen et al., 2001). A recently recognized type of fracture damage surrounding the surface trace of large active fault zones involves the in situ fragmentation of the protolith around the fault core, such as inferred from observations at several localities of the same fault (Reches and Dewers, 2005; Dor et al., 2006). The original structure and textures of the protolith are preserved, but pervasive microfracturing of the protolith has lead to complete incohesion. They have been termed 'pulverized' rocks.

2.2. Fault zone scaling and development

As summarized in the previous sub-section, fault zone structure depends on a variety of factors. Hence caution must be used in the scaling relations among fault zone characteristics such as fault thickness or damage zone width. This problem can be particularly acute when datasets from different areas are combined. The way in which different authors have defined damage zone width (mean width at one site, single measurement along a scanline or maximum damage zone width envelope) makes comparing studies very difficult (Shipton et al., 2006). Another issue is that the data may be biased by differences in the methods used to measure the fault "width" (e.g. should the "width" of the San Andreas fault zone as measured from a geological map or satellite photo include all the low-strain rock in between the various strands of the fault system?) (Schulz and Evans, 2000). Where faults with a range of displacements or lengths formed in the same protolith, at approximately the same depth and environmental conditions and under a similar stress field, then useful scaling relationships may be determined (e.g. Childs et al., 2009; Mitchell and Faulkner, 2009).

Faults initiate from the coalescence of a number of growing mode I cracks (Reches and Lockner, 1994; Healy et al., 2006). Commonly, the initiation of faults occurs on pre-existing planes of weaknesses such as cooling joints (Martel et al., 1988; Di Toro and Pennacchioni, 2005), dykes (d'Alessio and Martel, 2005) or tectonic joints (Wilkins et al., 2001; de Joussineau and Aydin, 2007; Moir et al., 2010).

As fault cores develop, wear models have suggested that progressive damage leads to the development of a wider fault core. Broad trends may be seen in fault core thickness – displacement relationships (Scholz, 1987), but the wide scatter in these data may reflect the fact that these compilations are from faults developed in wide range of tectonic regimes and which formed in variable environmental conditions. Although wear models are physically appealing from a mechanical perspective and make intuitive sense, the complexities arising in natural fault zones produce a wide range of resultant fault core internal structures (Evans, 1990; Shipton et al., 2006; Faulkner et al., 2008). In summary, quantitative models for fault core development may not be universally applicable and may, more accurately, provide an upper bound on fault core width.

The growth of fault damage zones and their scaling with fault displacement is an important topic, as the fracture damage zones surrounding faults may provide fluid flow pathways of economic significance and, in addition, act as an energy sink during quasi-static fault growth or dynamic rupture. Vermilye and Scholz (1998) made measurements of small displacement faults and concluded that fault damage zone width (defined by the points where fracture damage falls below background levels on either side of the fault) scales with fault displacement. Mitchell and Faulkner (2009) studied damage zone width defined by macro- and micro-fracture densities for faults developed within the same granodioritic batholith over nearly five orders of magnitude of displacement (Fig. 5). The damage zone width scales with fault displacement, however at higher displacements the rate of growth of the damage zone width with displacement decreases after a few hundred

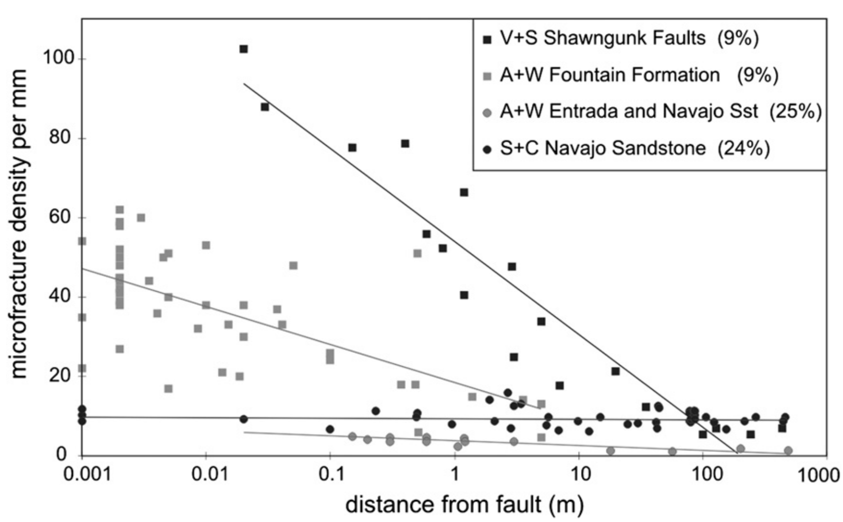

Fig. 4. Comparison of microfracture density with distance from the main fault from high porosity rocks with deformation bands (Anders and Wiltschko, 1994; Shipton and Cowie, 2001) with microfracture density from low porosity rocks (Anders and Wiltschko, 1994; Vermilye and Scholz, 1998). The average host rock porosity for each site is given in brackets. Linear regressions show that in low porosity rocks a logarithmic decay of microfracture density occurs with distance from the fault zone. Conversely, in high porosity rocks, microfracture densities drop to background levels at all points outside the fault zone.

metres of displacement (Fig. 5). Micarelli et al. (2006) found a similar decrease in the growth of fracture damage zone width at displacements above 1–5 m in high-porosity carbonate sequences in Sicily. However, in this case, displacements of 1–5 m coincide with the onset of cataclastic fault rock generation, which may be controlled by the scale of the bedding in these rocks which is of the same order of magnitude. Savage and Brodsky (submitted for publication) compiled fault width versus displacement data from a range of sources (with inherent limits of comparison) and also suggest that the growth of the macrofracture damage zone width decreases markedly for larger (>100 m) displacement faults.

Many authors have attempted to relate the fracture damage around faults and the width of the damage zone to the mechanics responsible for their formation. Such studies are particularly attractive for, if the underlying physics are understood, predictions of damage zone properties can be made for any faults where the mechanical properties of the protolith are known. Fig. 6 summarizes the primary processes that have been suggested for the production of fracture damage surrounding faults (Wilson et al., 2003; Blenkinsop, 2008; Mitchell and Faulkner, 2009). Many damage zone models have concentrated on the link to process zone mechanics (Anders and Wiltschko, 1994; Vermilye and Scholz, 1998) or the repeated slip on small patches along a single fault (Shipton and Cowie, 2003). The intensity of tensile damage can be related to slip distribution surrounding the fault tip (Savage and Cooke, 2010) or stress-release at extensional relays (Soliva et al., 2010). The various types of models have, in general, predictable fracture populations and orientations. However, many of the predicted fracture orientations are very similar and distinguishing between them is difficult. Given that many of these processes operate at various times on any given fault, the pattern of fracturing may be very difficult to interpret (Fig. 6f). The conclusions from most recent studies have supported the idea that the fracture damage surrounding faults accumulates from a combination of processes (Shipton and Cowie, 2003; Wilson et al., 2003; Blenkinsop, 2008; Mitchell and Faulkner, 2009).

2.3. Fault-system development

This review has largely concentrated thus far on the development of individual faults. This review has largely concentrated thus far on the development of individual faults. To understand the growth of faults and interpret relationships between displacement and length, or displacement and damage-zone development, we must also consider the interaction of faults or fault segments.

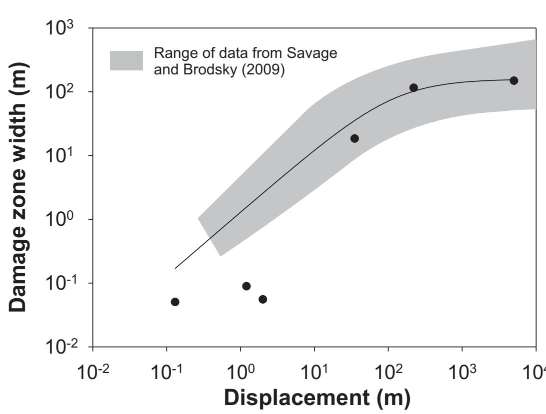

Fig. 5. The scaling of damage zone width (for both macrofractures and microfractures) as a function of displacement. The filled circles are microfracture damage zone data (collected from a single low porosity, crystalline lithology) from Mitchell and Faulkner (2009); the shaded area shows the extent of data compiled by Savage and Brodsky (submitted for publication) from a range of different faults, using macrofracture damage zones. The data from Mitchell and Faulkner are fitted with a hyperbolic function shown by the solid line.

For a fault zone with significant displacement, it is difficult or impossible to confidently identify the incremental steps which occurred during its development. Where syn-tectonic (growth) strata are preserved, however, the stratigraphic architecture of these units may provide constraints on the development of fault systems (e.g. Gawthorpe et al., 1997). For example, high-resolution 3D seismic surveys (e.g. Baudon and Cartwright, 2008; Lohr et al., 2008) image the geometry of growth strata. Additionally, numerical and analogue modelling allows systematic study of fault-zone and fault-system development with known boundary conditions (see papers by Henza et al., 2010; Moir et al., 2010; Schmatz et al., 2010).

As proposed by many authors (Walsh and Watterson, 1988; Peacock and Sanderson, 1991; Walsh et al., 2002; Childs et al., 2009), larger faults are the result of the growth and linkage of smaller faults. This growth and linkage process commonly produces a variety of fault-related folds, which are the continuous (ductile) deformation that accompanies and is genetically related to faulting (e.g. Anastasio et al., 1997; Cosgrove and Ameen, 2000; Wilkerson et al., 2002). Fault-related folds include folds that accommodate displacement variations on faults (e.g. relay ramps), folds resulting from fault-tip propagation, and folds due to movement on non-planar faults (which may form due to the linkage of non-coplanar fault surfaces). Fault-related folds are associated with reverse and thrust faults (Suppe, 1983; McClay, 2004; Shaw et al., 2005), normal faults (Schlische, 1995; Janecke et al., 1998; Withjack et al., 2002), strike-slip faults (Christie-Blick and Biddle, 1985; Harding, 1990) and oblique-slip faults (Tindall and Davis, 1999; Cristallini and Allmendinger, 2001; Schlische et al., 2002). The rock properties in these folds are commonly modified; thus, some fault-related folds may be considered as part of the fault's damage zone.

The formation of larger faults through the linkage of smaller faults influences scaling relationships (Dawers and Anders, 1995; Kim and Sanderson, 2005). For example, when two smaller faults link, the resultant length might be longer than if the fault grew as a single structure. Walsh et al. (2002) note that once some of the faults in a system become larger than others by segment linkage, they tend to dominate further deformation by increasing displacement rates; this typically results in the cessation of the activity on the smaller faults.

Early attempts to infer the scaling relationships of faults relied largely on log–log plots of maximum displacement versus length. These datasets indicate that similar displacement – length ratios occur for a wide range of scales, suggesting some scale-invariant behaviour to fault propagation and growth (Walsh and Watterson, 1988, also see Bonnet et al., 2001 for a review). The recognition of the importance of segment linkage in fault growth at least partially explained the wide scatter in the data, even on log–log plots (e.g. Cartwright et al., 1995; Dawers and Anders, 1995; Kim and Sanderson, 2005). Interestingly, analyses of the thickness of fault cores showed similar scale-invariant behaviour on log–log plots of displacement versus thickness (Section 2.2). In both cases, the validity of this approach for inferring the mechanics of fault growth or fault core-zone development (e.g. by wear or abrasion) is difficult because of the hazards of comparing datasets from different lithological and tectonic settings. Nevertheless, in the case of fault-length scaling, generalizations of data sets can provide useful upper limits to feasible displacement gradients which are important as rules-of-thumb for quality control of structural interpretations from seismic data, particularly in the case of spare 2D lines (Freeman et al., 2010).

In sedimentary basins, fault linkage typically involves the formation and eventual breaching of relay zones (see Walsh et al.,

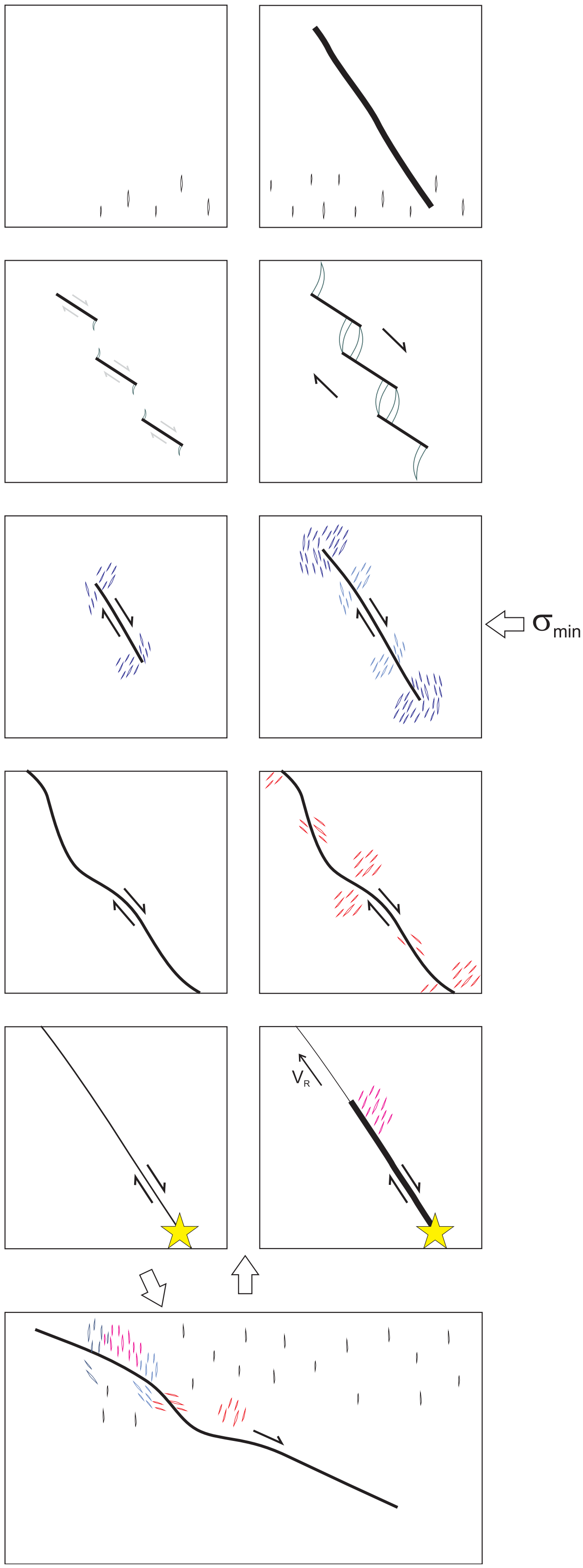

Fig. 6. Processes that are responsible for creating off-fault damage resulting in damage zones (after Mitchell and Faulkner, 2009). The damage in the figure is shown as mode I fractures surrounding a fault. Left-hand side boxes show the initial state and right-hand side boxes show a more evolved state. (a) Shows damage from the coalescence of microfractures; (b) shows damage from linking of structures (c) shows damage from fault growth involving a 'process zone' (d) shows damage from continued displacement on 'wavy' faults; (e) shows co-seismic fracture damage, where V_r is the rupture velocity and (f) illustrates how a combination of all these can produce a complicated pattern of fracture damage surrounding a fault core (based on work from Wilson et al., 2003; Blenkinsop, 2008; Mitchell and Faulkner, 2009). Note that damage generating processes highlighted in this figure can be active at different stages during the evolution of a fault zone.

2002 and references therein). Recent studies of overlap and relay zones have shown how, at a variety of scales, they may evolve into fault-bounded lenses as the deformation evolves and the two segments fully connect to form a single fault (e.g. Kristensen et al., 2008; Childs et al., 2009). Similarly, asperity bifurcation ("splaying") such as at zones of enhanced wall rock fracturing, and along-strike reconnection of these splays results in isolation of lenses of low-strain wall rock between the splays in a growing fault zone (e.g. Van der Zee et al., 2008). Both of these processes are controlled by heterogeneities of characteristic length scales ranging from grain size through bed (e.g. Wilkins and Gross, 2002; Soliva and Benedicto, 2005) and joint scale (Van der Zee et al., 2008) to structures such as "sidewall rip-outs" at the scale of strike-slip faults in the upper crust (e.g. Swanson, 2005). The scale of these might be controlled by variations in fault orientation, possibly due to fault linkage. Thus, in reality, fault thickness growth may occur by a number of discrete scale-dependent steps (Wibberley et al., 2008). Recent studies using geomorphology (Whittaker et al., 2008; Roberts et al., 2009), shallow seismic surveys (Bull et al., 2006) and numerical modelling (Cowie et al., 2006) have investigated the accumulation of slip at breached relays and the relationship between throw rate and the longevity of sip minima at linkage sites. These results have important implications for basin development and earthquake rupture propagation through fault linkage zones (Roberts et al., 2009; Walker et al., 2009).

3. Mechanics of fault zones and fault systems

Quantification of the mechanics of faulting and earthquakes comes from in situ crustal measurements, laboratory friction testing, field measurements and inversion of seismic data (Scholz, 2002). Relative mechanical properties (without quantifying the absolute stresses) may be derived from field observations and seismic data. Classic work conducted by Byerlee (1978) provides a range of friction coefficients under which fault slip should occur at crustal depths where brittle deformation dominates. A compilation of crustal stress measurements by Townend and Zoback (2000) has highlighted the general applicability of Byerlee's law. Similarly, an analysis of the dip of seismogenic normal faults indicate that they generally fall at the lower end of the range of friction values suggested by Byerlee (Collettini and Sibson, 2001), and a similar observation holds for seismogenic reverse faults (Sibson and Xie, 1998). In this section we highlight instances where crustal fault strength appears to vary considerably from the picture outlined above. The mechanics of the earthquake process is then addressed.

3.1. *'Weak' faulting*

Compelling observations indicate that some faults slip under anomalously low friction coefficients, much less than those predicted by Byerlee. The notion of weak faults derives mainly from the orientation of the fault plane with respect to the maximum principal stress. Weak faults are classified as those that appear to slip even when frictional lock-up is predicted by Byerlee's law. One issue relates to explaining continued slip on a fault rotated out of its ideal orientation. However, another problem is to explain how some faults appear to have formed at such a non-optimal orientation (e.g. Collettini and Holdsworth, 2004).

The debate surrounding the problem of weakness on large thrusts is probably the oldest of those regarding weak faults. The paradox is that the maximum fault area that a relatively thin thrust sheet can load without breaking up internally is much less than observed in natural examples. Hubbert and Rubey (1959) suggested a solution where basal friction can be overcome by high fluid pressure in the thrust fault zone. Price (1988) on the other hand, showed that the paradox is based on the assumption that slip occurs on all of the thrust surface simultaneously, whereas evidence from earthquakes suggests that thrusts, like other active faults, operate by the overall accumulation of displacement on slip patches on different parts of the fault at different times. Furthermore, thrust zones in crystalline basement show extensive evidence for fluid-enhanced reaction weakening, encouraging a change in deformation mechanism regime from frictional sliding to shear by diffusive mass transfer and/or crystalline plasticity (Wibberley 2005).On the topic of reverse faults, Sibson (2009) recently showed that normal faults on the eastern side of the Sea of Japan reactivated in a reverse sense, as the back-arc basin has started to contract, are unfavourably oriented with respect to the regional stress field, suggesting they are weak.

Another class of faults that may be viewed as weak are low-angle normal faults (Axen, 2007). The existence of these structures is still debated, but compelling recent geological and geophysical data support their occurrence. One example can be found in central Italy, where extension and uplift is migrating from west to east, and previously active extensional structures have been exhumed and are exposed on the Island of Elba. Geological evidence suggests that the Zuccale fault on Elba, currently in a low angle orientation ($\sim 10^{\circ}$), was active in this same position during movement. The evidence for this includes the formation of contemporaneous footwall conjugate extensional faults (Smith et al., 2007) and the orientation of original compressional structures and vertical opening mode extensional veins (Collettini and Holdsworth, 2004). Farther to the west, from the surface to depths around 8 km, Chiaraluce et al. (2007) imaged a microseismically active zone, the Alto Tiberina fault, oriented at a low angle. They interpret this to be a currently active low-angle extensional detachment, of which the Zuccale fault to the east is an ancient, uplifted example.

For strike-slip faults, the San Andreas fault in California is inferred to be 'weak' based on heat-flow data, seismological constraints and stress orientation. Early work showed that there was a conspicuous absence of any elevated heat flow from fictional heating that essentially limits the average shear stress on the fault to typical stress drops in earthquakes, 10–20 MPa (Brune et al., 1969; Lachenbruch and Sass, 1980). These data, combined with the observation that the angle between the maximum principal stress and the San Andreas fault is high (most latterly by Hickman and Zoback, 2004; Boness and Zoback, 2006), suggest that the fault moves under friction coefficients of ~ 0.2 or less. The interpretation and the quality of both the heat flow and the stress orientation data are controversial (see Scholz, 2006 and references therein). Results from the San Andreas Fault Observatory at Depth (SAFOD) provided more data close to the San Andreas fault at 3 km depth at the southern limit of the creeping section near Parkfield. These data suggest the fault is indeed weak, at least in the creeping section (Hickman and Zoback, 2004; Scholz, 2006).

Regardless of whether or not weak faults exist, the debate has driven a large body of work regarding the strength of faults in general. Laboratory studies have concentrated on the search for a weak mineral phase that might realistically be present over seismogenic depths in sufficient quantities to promote weakening. The frictional strength of most single phyllosilicate phases is less than predicted by Byerlee's law (Rutter et al., 1986; Logan and Rauenzahn, 1987; Morrow et al., 1992; Scruggs and Tullis, 1998; Bos and Spiers, 2001; Saffer et al., 2001; Saffer and Marone, 2003; Moore and Lockner, 2004; Tembe et al., 2006; Takahashi et al., 2007; Crawford et al., 2008; Ikari et al., 2009), although this is not always the case (van Diggelen et al., 2010). What is not so clear at present is how the mixing of weak clay material with other phases, such as quartz affects gouge strength, and how the fluid phase may affect whether sliding is dominated by friction or another, viscous, rheology. There are few studies that have addressed the first question, but those that have suggest a gradual decrease in frictional strength with the addition of clay (Takahashi et al., 2007; Crawford et al., 2008). It also appears that natural fault rock microstructures, with inter-connected networks of weak phyllosilicate phases, are important to produce some form of weakening (Holdsworth, 2004). Collettini et al. (2009a) compared the frictional strength of intact wafers of natural fault gouge from the Zuccale fault (Elba, Italy) to mineralogically identical powders and found the material retaining the in situ microstructure is significantly weaker than its powdered counterpart. This suggests that previous experiments where powdered natural gouge was used provide an upper bound on the strength at best. However, the experiments on single mineralogical components should still provide a useful guide to the lower strength bound for natural gouge containing these phases.

Phyllosilicate phases the required strength to explain 'weak' faulting, such as montmorillonite or chrysotile, tend to strengthen at laboratory pressures and temperatures greater than that equivalent to a few kilometres depth (e.g. Morrow et al., 1992; Moore et al., 2004). One exception is talc, which shows remarkable weakness over the entire temperature and pressure conditions of the seismogenic crust (see Fig. 7a; Escartin et al., 2008; Moore and Lockner, 2008). For this reason the discovery of serpentinites and associated talc within cuttings from the SAFOD borehole was significant (Moore and Rymer, 2007). However, it is not clear if the talc is concentrated in sufficient quantities or along narrow slip surfaces in the two currently active strands of the San Andreas fault at the SAFOD site. Testing of powdered cuttings from the SAFOD borehole (with inherent limitations, as noted above) showed that friction coefficients are lower than those predicted by Byerlee, but not sufficient to account for the observations of fault weakness (Tembe et al., 2006).

Similarly, the presence of talc in the Zuccale low-angle normal fault has been noted. It is explained by reactions involving dolomite and silica-rich fluids (Collettini et al., 2009b). However, frictional studies of powdered natural gouge from the Zuccale fault suggest that the friction coefficients are too high to explain movement, although these might represent an upper bound of strength as powdered samples were used (Smith and Faulkner, 2010). Similar results apply to other low angle normal fault systems (Numelin et al., 2007). More importantly, the discontinuous nature of the talc-rich fault gouge layers in the Zuccale fault show that, even with the presence of talc, the geometry cannot explain slip (Smith et al., 2007; Smith and Faulkner, 2010). In summary, although intrinsically weak minerals do exist within fault zones, it is currently unclear whether these can be the sole source of weakening.

Laboratory testing generally occurs at room temperature conditions and at strain rates that far exceed their natural counterparts for fault creep. One possible way to weaken faults is that additional mechanisms other than frictional ones are responsible for fault slip. These would only operate at much slower strain rates than those achievable in the laboratory (Gratier et al., 1999). The overall dominance of pressure solution creep over frictional processes in fault zones remains a possibility (Rutter and Mainprice, 1979). Geological observations of many faults suggest that the mineralogical changes during deformation in large faults

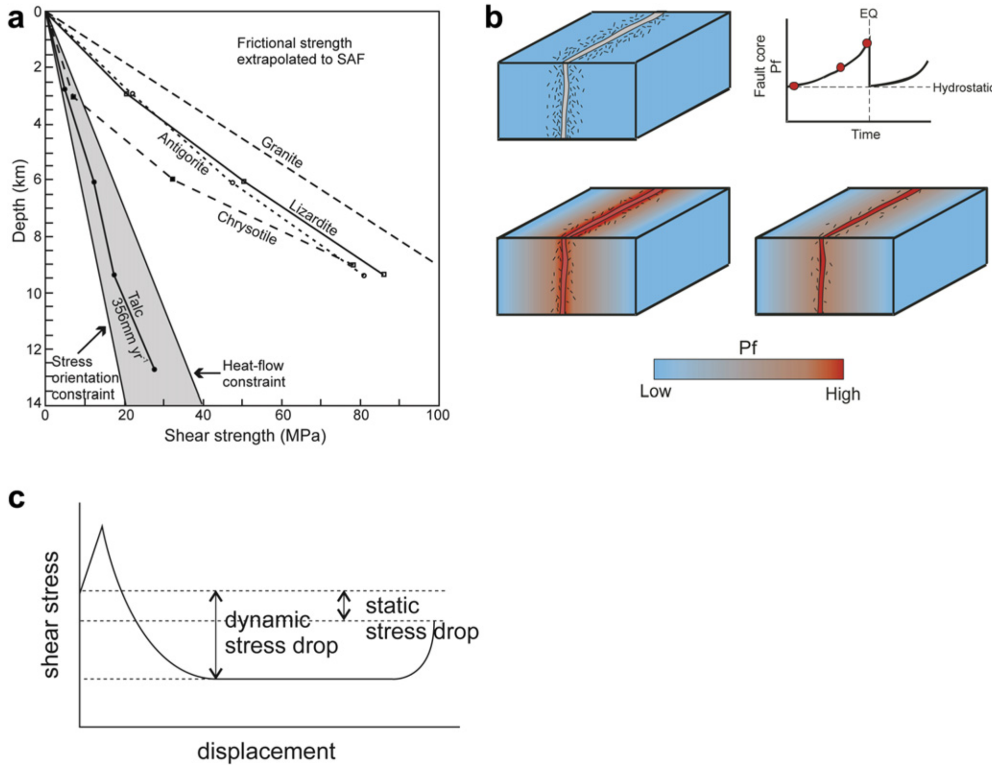

Fig. 7. Weak fault models. (a) Talc strength over the brittle crustal conditions. (b) An example of transient fluid pressure weakening based on a crack seal cycle (e.g. Byerlee, 1993); and (c) dynamic weakening, where the dynamic stress drop (not measurable in earthquake events) is much larger than the measured static stress drop, requiring that much less energy is dissipated in the earthquake than might be expected.

might promote this type of behaviour (Wintsch et al., 1995; Imber et al., 2001; Holdsworth, 2004). If pressure solution is operative in very mature fault zones, the soluble phases may be removed entirely, leading renewed frictional behaviour. Experiments on rock analogues (halite and clay) showed that both frictional processes and pressure solution are can operate simultaneously (e.g. Bos et al., 2000). One problem is that characteristic microstructures indicating that pressure solution creep was operative in natural fault rocks are difficult and sometimes impossible to find. Pressure solution experiments on natural rocks, or those that are likely to be present in natural fault zones, are few, and the diffusion rates for quartz, for example, are slow (Hickman and Evans, 1995; Gratier et al., 2009). Consequently it is difficult to assess the possible contribution of pressure solution creep on fault behaviour. However, if used to explain possible weakness, it will be more applicable to faults with low displacement rates (e.g. ~1 mm/year) such as those predicted for low-angle detachment faults, or in the interseismic period between earthquakes (e.g. Renard et al., 2000).

Another possibility for intrinsic fault weakening arises from the concentration of phyllosilicate phases in mature fault cores. Wintsch et al. (1995) suggested that a layer of well-orientated phyllosilicate basal planes might provide a weak horizon within faults. Experiments on phyllosilicates shows they have significant mechanical anisotropy (e.g. Mares and Kronenberg, 1993; Mariani et al., 2006 and references therein). Mariani et al. (2006) showed that with muscovite polycrystals at elevated temperature and very low laboratory strain rates deformation approached linear viscous and showed no grain size dependence, suggesting some form of Harper-Dorn creep. Clearly additional experiments at lower strain rates are necessary to investigate these processes further.

High pore fluid pressures are another mechanism that may weaken faults (Fig. 7b; Hickman et al., 1995). One model involves pore pressure that varies over the seismic cycle. Immediately following an earthquake the permeability of the fault is high (Sibson, 1990). Over time, permeability falls and compaction of the fault leads to overpressure and promotes slip (Blanpied et al., 1992; Byerlee, 1993). A second model involves a fault zone that continuously acts as an impermeable barrier and high pore fluid pressure is maintained by a fluid flux from mid-crustal levels (Byerlee, 1990; Rice, 1992). The first model is more applicable to seismogenic faults, where as the second is better suited to faults undergoing creep. Geological evidence supports both models. For the second model, low permeability fault gouges and a favourable fault zone structure suggests that long term sealing is possible if fluid sources at depth are available (Faulkner and Rutter, 2001). One drawback with these models is that the level of pore fluid pressure required to promote slip on very unfavourably oriented faults generally exceeds the minimum principal stress (Rice, 1992). Thus, the pore pressure would always be limited by hydrofracturing and fluid pressure loss before slip occurs on the fault. This problem is circumvented if the stress state within the fault zone is different to the remotely applied stress field. This condition is possible, with mechanical continuity, if the mechanical properties of the fault zone are different from the country rock (Rice, 1992; Chery et al., 2004; Faulkner et al., 2006).

One final fault weakening mechanism operates during seismic slip (dynamic weakening; Fig. 7c). If operative, dynamic weakening mechanisms can explain the lack of any heat flow anomaly but, in the absence of any other weakening mechanism, cannot explain the nucleation of dynamic events on a severely misoriented fault. The issue of dynamic rupture will be discussed in Section 3.3.

3.2. Earthquake nucleation

The issue of how earthquakes nucleate is important because it might produce measurable precursory phenomena that may be used in short-term earthquake prediction (Ellsworth and Beroza, 1995; Beroza and Ellsworth, 1996). In recent years, modelling of the build up to instability has generally utilized the rate- and state-dependent friction laws that predict a period of stable, aseismic slip preceding instability. The rate and state formulation also allows a wide variety of observed fault behaviour to be modelled including aseismic fault creep, slow earthquakes and dynamic rupture (Scholz, 1998).

The principles of rate and state friction are well-known and are only briefly described here (for reviews on rate and state friction behaviour see Dieterich and Kilgore, 1996; Marone, 1998). Although extrapolated to accelerating slip and instability in the case of earthquakes, the formulation is based on laboratory experiments where the response of the dynamic friction coefficient to a step increase sliding velocity is measured (see Fig. 8). There is an instantaneous response of the friction coefficient (or equally the shear traction) to the change in velocity (the rate effect), followed by time-dependent evolution over a particular slip displacement (the state effect) (Fig. 8). The rate and state friction law (Eq. (1)) is purely phenomenological and the physical processes responsible for the observed behaviour, particularly for the state evolution, are poorly known.

$$\mu = \mu_0 + a\ln\left(\frac{V}{V_0}\right) + b\ln\left(\frac{V_0\theta}{D_c}\right) \tag{1}$$

where μ and μ_0 are the friction coefficient and the initial friction coefficient respectively, a and b are experimentally derived constants, V and V_0 are the new sliding velocity and the initial sliding velocity respectively, θ is the state variable and D_c is the slip weakening distance.

The evolution of the state variable is a function of time, normal stress and displacement and has units of time. It has been explained in terms of the 'age' of the load-supporting contacts and the time required for a new set of contacts to develop following a perturbation of the system (e.g. displacement rate, change in normal stress, etc.). Dieterich and Kilgore (1994) showed direct evidence that the state variable is related to the evolution of the area of the load supporting contacts over time and various normal stresses, termed 'asperity creep'. Two formulations are widely used to model the state evolution, the 'aging' (or 'slowness') law and the 'slip' law (Eqs. (2) and (3)).

$$\dot{\theta} = 1 - \frac{V\theta}{D_c} \text{ (Aging, Dieterich or Slowness law)} \tag{2}$$

$$\dot{\theta} = -\frac{V\theta}{D_c}\ln\frac{V\theta}{D_c} \text{ (Slip or Ruina law)} \tag{3}$$

These two formulations produce quite different styles of nucleation and rupture (e.g. Ampuero and Rubin, 2008).

The range of geological materials that have been characterized in a rate-and-state framework are few. Most comprehensive studies involve quartz and crushed granite powders. These granular materials generally show velocity weakening behaviour (where $a-b$ is negative, see Fig. 8) at low slip rates, opening the possibility for unstable slip (Green and Marone, 2002). Most natural fault zones contain at least a proportion of phyllosilicate minerals but experimental studies on these materials are even sparser (Morrow et al., 1992; Scruggs and Tullis, 1998; Reinen, 2000; Saffer et al., 2001; Moore and Lockner, 2008; Ikari et al., 2009; Smith and Faulkner, 2010). These studies generally suggest that phyllosilicate-rich gouges exhibit velocity strengthening behaviour at low slip rates (where $a-b$ is positive) and thus may be associated with fault creep (Faulkner et al., 2003). Talc, in particular, exhibits inherently stable, velocity-strengthening behaviour under all conditions tested (Moore and Lockner, 2008), although these conditions do not include seismic slip speeds ($\sim$0.1 to 1 m/s). Note, however, that montmorillonite and serpentinite gouge can both exhibit velocity weakening behaviour (Reinen, 2000; Saffer et al., 2001). Indeed, a recent compilation of experimental work suggests that even materials which exhibit velocity-strengthening behaviour at lower slip rates become velocity-weakening above $\sim$0.1 m/s (Wibberley et al. 2008). Some experimental studies have shown that phyllosilicates can exhibit negative b values (Saffer and Marone, 2003; Ikari et al., 2009; Smith and Faulkner, 2010), which are difficult to interpret physically as a negative b value is generally assumed to indicate an increase in contact surface area with faster slip. Karner et al. (1997) and Blanpied et al. (1998) also report negative b values for granular quartz and granite.

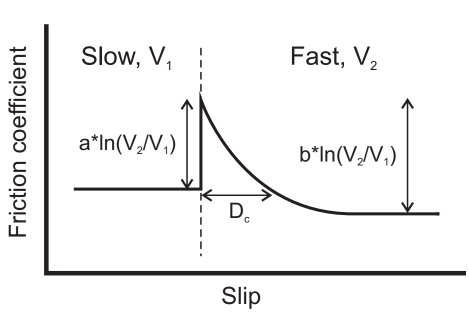

Fig. 8. Idealized rate- and state-dependent frictional behaviour, in which the mechanical response is defined by a stepwise change in velocity.

The microphysical processes responsible for the observed rate- and state-dependent behaviour are thermally activated and follow Arrhenius-type behaviour (Chester, 1994; Blanpied et al., 1998; Nakatani, 2001; Rice et al., 2001). They presumably include sub-critical crack growth, crystal plasticity, diffusion and possibly reaction at grain contacts. However, the rate and state formulation does not include temperature. Chester (1994) showed that the activation energy required for wet quartz gouge was consistent with sub-critical crack growth at asperity contacts. This is supported by the conclusions of Frye and Marone (2002) that relative humidity plays a role in the granular friction of quartz and alumina as a result of chemically assisted mechanisms. This is clearly an important area for future research, for if the physical mechanisms responsible for frictional behaviour are known and characterized, then the behaviour at a wider set of environmental conditions can be better predicted. However, we note that future progress in this area of research probably needs to combine experiments with detailed microscopy (SEM and TEM) and theoretical and computational studies due to the complexity of the interactions that occur at the nanoscale (Szlufarska et al., 2008; Mo et al., 2009).

3.3. Mechanics of dynamic rupture

The properties of faults during rupture are typically studied using inversion of seismic data recorded during earthquakes to compute the slip distribution of rupture events (kinematic model). Various models allow computation of the stress field, from which the physical properties of the rupture are inferred (see review by Kanamori and Brodsky, 2004). Recently, complementary laboratory studies and field measurements have led to a better understanding of dynamic rupture, although this is currently a rapidly developing area of research.

The slip history during large earthquakes appears to take the form of a slip pulse rather than a self-similar crack-like rupture (Heaton, 1990). In the slip-pulse model, only part of the fault plane ruptures at any one time. Most seismological models now assume source-time functions of small finite duration and thus implicitly apply the slip-pulse model. However, this mode of slip still raises a number of unanswered questions. First, the spectral signature of large earthquakes suggests that the corner frequency (lowest frequency seismic waves) scales with rupture area which runs contrary to the idea of a similar-size slip pulse regardless of the size of the rupture. Additionally, in the early stages of failure the slip-pulse model must accumulate approximately the correct amount of slip appropriate to the overall rupture size. This leads to the question of whether an earthquake event knows *a priori* how large it will be (Marone and Richardson, 2006). Finally, modelling using a rate-and-state framework has shown that slip pulses can only develop under a restricted set of conditions where the initial shear stress on the fault is low (Zheng and Rice, 1998). Low stress ('weak') faults might well exist (Section 3.1), but a large proportion of faults are inferred to have 'high' stress levels (Townend and Zoback, 2000). Does this mean that slip pulse-type behaviour is not possible for these faults?

Seismic records allow modelling of the mechanical properties of rupture, but, in recent years, laboratory and field measurements have provided independent constraints. All these data yield an understanding of the rupture process in terms of the energy balance for an earthquake (Eq. (4); see Kanamori and Rivera, 2006). The change in potential energy ΔU_e (the sum of the elastic strain energy and gravitational energy during earthquake slip) is the sum of surface energy U_s (to produce new crack surface area), kinetic energy U_k (radiated as seismic waves) and frictional energy U_f (dissipated as heat):

$$\Delta U_e = U_s + U_k + U_f. \tag{4}$$

Constraints on the kinetic energy are well known from modelling of seismic waves. Chester et al. (2005) estimated the fracture energy for the Punchbowl fault in California by accounting for all the fracture surface energy in both the damage zone and, more importantly, the core zone, where nano-sized particles are present and account for a significant proportion of the fracture area. Hertzian fracture models (where fracturing occurs at grain contacts of spherical grains) suggest that it is mechanically very difficult to produce such small particle sizes. Sammis and Ben-Zion (2008) suggested that shock loading and sub-critical crack growth under compressive stress, or high strain rate tensile stress may be responsible. The fracture energy expended during the formation of 'pulverized rocks' (Section 2.1) that are thought to develop during seismic slip near the surface is not currently known. However, Biegel et al. (2008) showed that off-fault damage will affect the velocity of an earthquake slip pulse.

Di Toro et al. (2005) showed that a simple analysis of pseudotachylyte veins provides broad constraints on the dynamic stress during rupture. This analysis indicated very low (in terms of Byerlee friction) shear stresses driving rupture. Di Toro et al. (2006) corroborated these results with measurements, using the same protolith, of dynamic friction at seismogenic slip velocity. While frictional melting might result in low shear stresses driving slip (after the effects of viscous braking have been overcome; Tsutsumi and Shimamoto, 1997), the friction of other granular materials at high velocity were unknown until recently.

Technical developments over the past 15 years (notably in the laboratories of Shimamoto and co-workers) have allowed measurement of the stresses during high-velocity frictional testing in rotary shear apparatus. Fig. 9 shows typical results from a friction experiment conducted at seismogenic slip velocity. These data complement the data modelled from natural earthquake ruptures. A key feature of the data in Fig. 9 is the dramatic weakening from Byerlee levels of friction down to levels between 0.1 and 0.2. The reasons for this weakening are many, and dependent on the material tested. They include flash heating at asperity contacts (Bowden and Tabor, 1950), silica gel formation (Goldsby and Tullis, 2002), thermal pressurization (Hirose and Bystricky, 2007), frictional melt lubrication (Di Toro et al., 2006) and thermal decomposition (Han et al., 2007). Recent modelling of the earthquake process has started to combine and incorporate some of these additional thermal factors into rate- and state-frictional frameworks (Rempel and Rice, 2006; Rudnicki and Rice, 2006; Segall and Rice, 2006; Noda, 2008; Noda et al., 2009).

The results in Fig. 9 have important implications. First, they explain the long-standing debate on the development of frictional melting in fault zones. Simple analyses show that extreme temperatures are quickly reached due to frictional heating (see Rice, 2006 for a summary). All these models assume friction coefficients commensurate with Byerlee's law. If the shear traction required for seismic slip reduces dramatically then the frictional energy converted to heat is also dramatically reduced. It can also explain the lack of any heat flow anomaly (Section 3.1) over the seismogenic parts of the San Andreas fault.

Another feature of high velocity laboratory tests is the magnitude of D_c which is on the order of decimetres to metres. In slow frictional testing (Section 3.3) to determine rate- and state-friction parameters, the slip-weakening distance is on the order of microns. A long-standing debate focuses on the apparent discrepancy of D_c values derived from the laboratory versus values inferred from seismological data, the latter being on the order of a metre. This parameter may scale with fault roughness or fault thickness (Scholz, 1988; Marone and Kilgore, 1993). The emergence of models that account for the different physical processes that occur during seismic slip as opposed to slow laboratory frictional sliding seem to provide an answer to the discrepancy. It appears the seismically derived D_c is a different parameter to that measured at slow slip rates in the laboratory, and involves fundamentally different physics. This is supported by the range of behaviour observed in high velocity experiments, modelling and from other geological observations that include thermal pressurization (Wibberley and Shimamoto, 2005; Bizzarri and Cocco, 2006), flash heating, thermal decomposition and frictional melting. The value of D_c might be envisaged to increase as thermally activated processes continue to produce weakening with continued slip (in the same way that the boundary between surface energy and heat varies during slip as suggested by Tinti et al., 2005). It is clear that smaller critical slip distances must exist, otherwise small earthquakes could never nucleate and that a sensitive balance exists between the energy required for the work of fracture and that converted to heat. Unfortunately, testing these hypotheses with seismological data is hampered by the limited frequency bandwidth from which kinematic models of rupture are derived and also the constraints on the resolution and uniqueness of

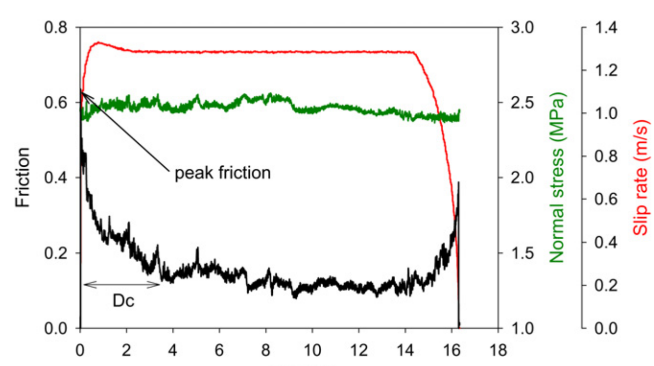

Fig. 9. Results from a typical high-velocity friction experiment on kaolinite (unpublished data from Faulkner, Mitchell, Hirose and Shimamoto). It shows a number of characteristic features including the peak friction, slip weakening distance and steady-state sliding. The strength recovery upon deceleration of slip is also shown.

parameters such as D_c (Spudich and Guatteri, 2004; Tinti et al., 2009). Field observations by Kirkpatrick and Shipton (in press) confirm that slip weakening mechanisms are likely to be spatially and temporally variable across an earthquake fault surface.

4. Fluid flow in fault zones

In recent years our understanding of fluid flow through faults has advanced greatly. The typical structure of fault zones (Section 2.1), with a core and damage zone, has provided the framework within which to place laboratory measurements of the fluid flow properties of natural and synthetic fault products into context (Fig. 10). Fault-related fluid flow has also been investigated via a number of indirect data sources such as migrating seismicity at depth, shallow reservoir-induced seismicity, springs, geysers and geothermal systems. These sources have provided some first-order constraints on the rates of fluid flow in natural fault zones at depth, and at length scales unavailable to lab experiments.

In the original Caine et al. (1996) fault core and damage zone model of fault architecture the fault core was visualised as providing an across-fault barrier to flow and the fractured damage zone as an along/up-fault conduit. However, the varying fault architectures outlined in Section 2.1 gives rise to a much more complex set of fault zone hydraulic behaviours. The intricate structure of low and high permeability features within a fault zone can lead to extreme permeability heterogeneity and anisotropy. The permeability of a fault zone, both in-plane and perpendicular to the plane (across-fault) is governed both by the permeability of the individual fault rocks/fractures and, critically, by their geometric architecture in three dimensions (e.g. Lunn et al., 2008). For example, rocks from the fault core are commonly rich in phyllosilicates, which typically have low permeability, but only form barriers to flow if they are continuous throughout the fault plane (Faulkner and Rutter, 2001). Open fractures and slip surfaces (both within the fault core and the surrounding damage zone) have a permeability governed by their aperture distribution, which is in turn influenced by their orientation to the present day local stress field. Such fractures and slip surfaces may have a substantially greater permeability than the host rock; however, their net effect on bulk along-fault and across-fault flow, depends entirely on their connectivity and ability to cross-cut other lower permeability units.

4.1. The hydraulic properties of the fault core and its influence on fluid flow

In natural faults two distinct types of gouge are present. The first are granular materials composed of broken, irregular but roughly equant clasts (in the sense that their long and short axes are approximately equal), and the second are gouges that contain some proportion of phyllosilicate material. Relatively few data on the permeability of 'granular' gouges are available but they tend to develop a characteristic grain size distribution (Sammis et al., 1987; Marone and Scholz, 1989) that may suggest a similar permeability development for all these materials. Zhang and Tullis (1998) measured the permeability development in synthetic quartz gouge at a normal stress of 25 MPa. They found that at shear strains up to $\sim$10 the permeability is reduced by two to three orders of magnitude. This is in agreement with more recent findings of Crawford et al. (2008) and Main et al. (2000). Beyond this shear strain (to a shear strain $\sim$200), Zhang and Tullis (1998) found the permeability dropped by a further two to three orders of magnitude and that a permeability anisotropy of one order of magnitude developed. This was due to the formation of localized, fine-grained Y shears. These laboratory data are in agreement with field observations and permeability measurements from boreholes that suggest a significant drop in cross-fault permeability in deformation band-dominated faults as the fault core develops throughgoing slip surfaces (Shipton et al., 2002, 2005).

Fault zones rich in phyllosilicate material tend to have lower permeabilities than quartz and/or framework silicate-rich gouges. Information on the fluid flow properties of phyllosilicate-rich fault zones is necessary to understand fluid flow associated with fault creep (e.g. Faulkner and Rutter, 2001) and earthquake slip (e.g. Wibberley and Shimamoto, 2005; Yamashita and Suzuki, 2009), as many large faults contain significant proportions of clays. Where the fluid-flow properties of fault zones are needed to evaluate the robustness of a fault-bounded hydrocarbon prospect or the field compartmentalizing effects of intra-reservoir faults, estimating the possible phyllosilicate content of the fault zone is critical, along with reservoir juxtaposition geometry. Based on field-observations of fault zones, the two main mechanisms that entrain phyllosilicates (typically shale and/or clays) into fault zones in layered sandstone – shale sequences are shale or clay smearing (e.g. van der Zee and Urai, 2005) and abrasional mixing (e.g. Yielding et al.,

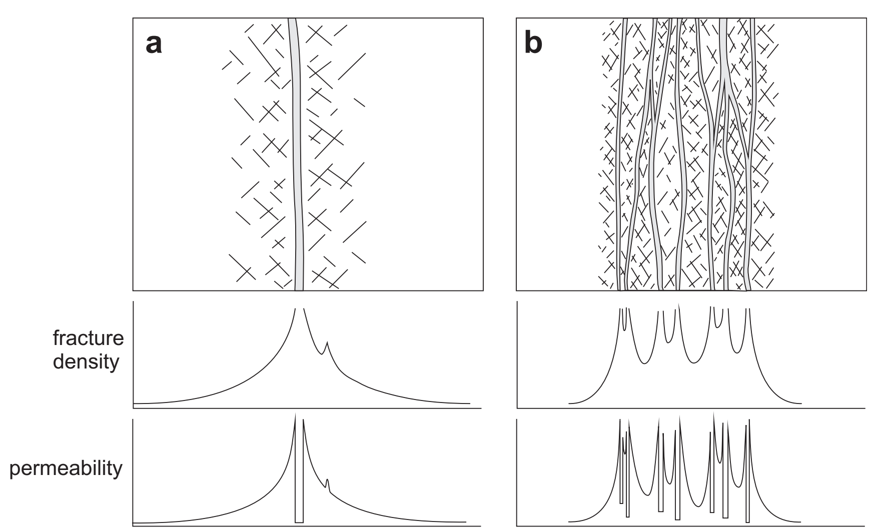

Fig. 10. Some physical properties of fault zones related to their structure (damage zone and fault core). (a) Single fault core and (b) multiple fault core, which illustrates the resulting complexity in characterizing the resultant properties.

1997). The necessity of estimating fault properties from limited datasets led to algorithms for estimating fault zone composition which assume one or the other mechanism is operative. For shale/clay smearing, the Clay Smear Potential (Weber et al., 1978) or the Shale Smear Factor (Lindsay et al., 1993) rely on parameters such as the thickness of the shale/clay source bed, distance of a point on the fault from that source bed, and/or throw. These algorithms only predict whether or not the smear along the fault is discontinuous (likely leading to leakage) for a given fault throw and, if so, where. On the other hand, the abrasional mixing mechanism led Yielding et al. (1997) to propose the Shale Gouge Ratio (SGR) algorithm, a ratio or percentage of shale in a silicilastic fault zone, which simply assumes that any one point on the fault has a composition identical to the average composition of the sequence past which that point has slipped. In terms of sandstone – shale sequences, this is extremely practical to implement, because the net volume of clay (Vcl) logs from nearby wells can be extrapolated onto the fault (in cases of simple stratigraphy), from which SGR is calculated for all points on the fault for which wall-rock Vcl data exist. In reality, fault zones are much more complex and local small-scale variations can exist even in abrasive fault zones where the rule generally holds. However, quantitatively constraining this variation may in future help predict uncertainties in SGR-based evaluations.

In evaluating the sealing potential of a fault, analysis of juxtapositions of reservoir/carrier beds against other reservoir beds is critical. Basic geometric evaluation of such likely leak points is easily done by fault-plane mapping of hanging-wall / footwall juxtapositions, commonly called Allan diagrams (Allan, 1989). However, field-based studies show that faults are commonly both segmented (in both dip and strike, e.g. Nemser and Cowan, 2009), have multiple slip surfaces and involve varying degrees of ductile deformation (fault-related folding; Section 2.3). Thus the net throw observed on one fault at the scale of seismic resolution is in reality often divided over two or more slip surfaces which share the displacement at the sub-seismic scale. Such fault zone structure therefore implies there might be reservoir-reservoir juxtapositions across individual fault strands even where the entire fault completely offsets the reservoir. Thus, better prediction of the likely segmentation and slip zone bifurcation is needed, particularly the incorporation of lenses of host-rock into the fault zone (e.g. Van der Zee et al., 2008, Schmatz et al., 2010).

The recognition that fault zones in siliclastic sedimentary basins are typically sand-shale gouges with fluid barrier/transmission behaviour governed by similar principles as shale-rich top-seals, led to the application of capillary sealing theory. By using calibration data for given fault-rock clay compositions and using laboratory measurements (e.g. Sperrevik et al., 2002) or field post-mortem results (e.g. Bretan et al., 2003), the SGR method can be used to map estimated capillary threshold pressures on the fault, yielding the likely maximum hydrocarbon column height trapped against the fault. The more recent recognition that fault zone heterogeneity may lead to connected “weak points” which may provide a pathway for hydrocarbon leakage has emphasized the need to predict better the variability in fault zone structure and composition.

Similarly, fault zone permeability, particularly for incorporating fault impact into reservoir simulators via the transmissibility multiplier (Manzocchi et al., 1999), is commonly estimated from SGR – permeability algorithms. Generally, there is a non-linear dependence of the permeability on the fault zone clay content under hydrostatic conditions due to the grain size difference and compaction characteristics. For example, as the clay content increases to between 25 and 40 volume % (the theoretical porosity minimum, Revil et al., 2002) the clay particles sit in the pore space between quartz, and the compaction characteristics are largely controlled by the quartz framework. The permeability is strongly controlled by the fraction of clay (Takahashi et al., 2007; Crawford et al., 2008). At larger percentages of clay, the permeability is less sensitive to the magnitude of the clay fraction. As the clay compacts more readily than the quartz, the porosity minimum varies with effective pressure (Crawford et al., 2008). Shear-enhanced compaction is much less pronounced for the clay component than for the quartz end-member. As a result, the clay-rich mixtures do not reduce their permeability by much in comparison to the quartz-rich gouges, which undergo a significant permeability reduction (Takahashi et al., 2007; Crawford et al., 2008).

Many measurements of natural clay-rich fault rocks are available (Faulkner and Rutter, 2000; Faulkner et al., 2003; Wibberley and Shimamoto, 2003; Tsutsumi et al., 2004; Mizoguchi et al., 2008). They all demonstrate the very low permeability of this material. Natural gouge can have permeability anisotropy of up to three orders of magnitude (Faulkner and Rutter, 2000). For synthetic phyllosilicate gouges this value appears to be much lower (Zhang et al., 1999), presumably due to the nature and distribution of the authigenic clay phases that develop in natural gouges. Recent work has measured the intensity of clay fabrics by, for example, X-ray texture goniometry (Solum and van der Pluijm, 2009; Haines et al., 2009). The gouges have a generally weak preferred orientation of the clays. Solum and van der Pluijm suggest that this indicates that the clay fabrics are localized phenomena. Haines et al. (2009) imply that the lack of clay fabric indicates the permeability anisotropy must also be low. However, previous work on clay fabrics shows that the permeability anisotropy is not due to clay alignment; indeed this can only account for a permeability anisotropy less than an order of magnitude (Faulkner and Rutter, 1998). Alternating microlayers of porous ‘granular’ material and fine grained clay-rich material are observed in the microstructure and explain the anisotropy (Faulkner and Rutter, 1998; Faulkner, 2004). Furthermore, authigenic clay growth observed in TEM images shows growth randomly in pore space in the stress shadows of larger relict grains (Rutter et al., 1986).

The pressure dependence of the permeability is remarkably similar for most clay-rich fault gouges, whether synthetic or natural (see Faulkner, 2004). Faulkner and Rutter (2000, 2003) showed that temperature and pore fluid chemistry can strongly affect the permeability of natural clay-rich rocks by altering physico-chemical interactions between the rocks and aqueous pore fluid.

The stress history of fault gouge, particularly clay-rich gouge, has been shown to be an important control on the permeability. Bolton et al. (1998) and Zhang et al. (1999) have shown that permeability is reduced in sheared gouges that have undergone normal consolidation, but may increase their permeability if they have undergone overconsolidation and are subsequently sheared at lower effective pressure conditions. Indeed the log-linear relationship of both porosity and permeability with mean effective stress in clay-rich gouges from the Median Tectonic Line, Japan, and dependence on the anisotropy of the stress regime suggest that fluid flow modelling in such fault zones may be based around a Cam Clay -type soil mechanics framework (Wibberley et al., 2008).

The temporal evolution of the permeability of fault gouges, particularly at hydrothermal conditions, has been a recent focus of research. Pure quartz gouges (Nakatani and Scholz, 2004a; Yasuhara et al., 2005; Giger et al., 2007) and quartzofeldspathic mixtures (Olsen et al., 1998; Tenthorey et al., 1998; Morrow et al., 2001) have been tested experimentally. Permeability reduction is found to be initially rapid and progressively slows with time. The rate of permeability reduction increases with increasing temperature (Olsen et al., 1998; Tenthorey et al., 2003; Nakatani and Scholz, 2004a; Yasuhara et al., 2005; Giger et al., 2007). The processes responsible for the permeability reduction are interpreted to be solution-precipitation processes (Nakatani and Scholz, 2004a;

Giger et al., 2007) and also precipitation of authigenic minerals following the breakdown of quartz and feldspar (Tenthorey et al., 1998). These processes have been successfully modelled (Aharonov et al., 1998; Nakatani and Scholz, 2004b). These studies have demonstrated that sealing will occur on time scales commensurate with those of earthquake recurrence times (Morrow et al., 2001).

4.2. Damage zone permeability

The permeability of fault damage zones is governed by the host-rock permeability and the presence and geometric composition of both macro-scale fracture networks (which will increase permeability), and of low permeability deformation and compaction bands (which will decrease permeability). Fault damage zone permeability in low porosity rocks (Balsamo et al., 2010) is generally fracture-dominated and governed by the connectivity of the macro-scale fracture network (Fig. 10). This contrasts with high porosity rocks where the damage zone may be more complex and permeability is governed by the frequency and connectivity of both low permeability deformation bands and of high permeability slip surfaces (Lunn et al., 2008). Both macro-scale fracture networks and deformation bands have been shown to decrease in frequency with increasing distance from the fault core (Rawling et al., 2001; Shipton et al., 2002; Wilson et al., 2003; Mitchell and Faulkner, 2009). Wibberley and Shimamoto (2003) measured the permeability of rocks collected from the surface trace of the Median Tectonic line in Japan. Their measurements showed permeability variations over several orders of magnitude, which can be explained by the lithological variation of the fault zone and also the structural complexity. Fig. 10 shows how this structural complexity might result in permeability heterogeneity from the variation in microfracture densities observed around multiple fault cores.

The permeability of the host rock within the damage zone is controlled by the frequency and orientation of microfractures. One potential problem with direct measurement of damage zone permeability from rocks collected from the surface outcrop of fault zones is that they may be subject to weathering or modification since the fault related microfracture network was produced (Morrow and Lockner, 1994). Measurements of rocks recovered from depth from fault-zone drilling projects may overcome this problem.

Experiments indicate permeability of initially low porosity rocks taken to failure increase by two to three orders of magnitude (Simpson et al., 2001; Oda et al., 2002; Uehara and Shimamoto, 2004; Mitchell and Faulkner, 2008). For initially high porosity rocks, the permeability may significantly decrease with deformation in the damage zone (Main et al., 2000). Measurements of permeability from the intact state of rocks to their failure stress can be scaled to the levels and distribution of damage seen surrounding fault zones (see Section 2.1), if a common factor between the two can be found. For example one such common factor is the microfracture density which can be measured in the field and then compared to that in experiments at various stages of damage, where the permeability may be readily measured.

4.3. Estimating bulk fault zone permeability

The physical characteristics of fault damage zones are described in Section 2.1. Estimates of the bulk fault zone permeability, for fault-perpendicular and fault-parallel flow, are derived from numerical models that simulate flow through the fault zone (Brown and Bruhn, 1998; Jourde et al., 2002; Matthai and Belayneh, 2004; Odling et al., 2004; Lunn et al., 2008) Such models show significant channelling of flow within fault zones into a small number of focussed flow paths. Similar channelling effects are observed in flow experiments within individual fractures (Brown et al., 1998; Beeler and Hickman, 2004). Observations from boreholes that penetrate faults, as well as along-fault and across-fault pumping tests, are necessary to determine bulk fault-zone permeability and to validate numerical models (Evans et al., 2005; Medeiros et al., 2010).

Very few studies have measured bulk fault zone permeability directly using boreholes. However, a number of secondary data sources allow estimation of along-fault permeability. Talwani et al. (1999) estimated the permeability of a shallow fault zone using sinusoidal pressure oscillations in boreholes from lake level fluctuations. Their analysis shows fault zone permeability, in faults that are subject to reservoir-induced seismicity, are between 1.1×10^{-15} and 1.78×10^{-15} m^2. Tadokoro et al. (2000) estimated along-strike fault (damage) zone permeabilities around $1–10 \times 10^{-15}$ m^2 from the migration rates of induced seismicity during borehole injection experiments in the Nojima fault zone following the Kobe 1995 earthquake. At deeper levels, Shapiro et al. (1997) found crustal permeability to be $\sim 10^{-16}$ m^2 in the KTB borehole in the depth interval 7.5–9 km. A compilation of fault zone permeabilities derived from reservoir-induced seismicity data can be found in Talwani et al. (2007). Using the same techniques of migrating patterns of seismicity, but at deeper levels in the brittle crust, Miller et al. (2004) estimated fault zone permeability to be 4×10^{-11} m^2 immediately following the M6 Colfiorito earthquake sequence of 1997 in central Italy. Noir et al. (1997) inferred a higher fault zone permeability of 10^{-8} m^2 for the Dobi earthquake sequence in Afar in 1989.

4.4. Spatial and temporal variability of fault zone permeability

A number of recent studies have shown that fault zone permeability is highly heterogeneous both spatially and temporally. Studies examining the distribution of geothermal spring temperatures along the Borax Lake fault, Oregon, USA, show that neighbouring springs a few metres apart can have widely different temperatures (Fairley and Hinds, 2004). These springs suggest that high permeability pathways exist as discrete structures in the Borax fault damage zone, and that individual flow paths have the capability to transport fluids rapidly from depth parallel to the fault plane. Dockrill and Shipton (2010) use observations of natural leakage of CO_2 along faults in Utah, USA, to show that along-fault flow is occurring at a few discrete locations along strike, and that these discrete along-fault flow channels have migrated over time. The presence of a modern oil seep at one location on the fault also indicates the existence of discrete unconnected along-fault ‘pipes’ that provide pathways for fluid flow from lithologies at depth to the surface and are unconnected to shallower horizons. Evans et al. (2005), during an injection test in the Soultz borehole, observed that “some 95% of the flow entered the rock mass at just 10 major flowing fractures”. Do Nascimento et al. (2005) show that pressure changes as low as 0.5 kPa (equivalent to 5 cm of water head) are enough to trigger transient changes in permeability that are spatially correlated, and related to seismicity below a water reservoir.

In the hydrocarbon exploration and production industry, evidence for the spatial and temporal variation of fault permeability exists but is usually limited to indirect inferences from reservoir fluid and pressure data either side of the faults, because faults are generally avoided when drilling as they give rise to a number of drilling problems (e.g. Grauls et al., 2002). Nevertheless, studies of charge timing in fault-bounded blocks (e.g. Residual Salt Analyses of fluid inclusions in reservoir pore cements) can show an increase in the hydrocarbon buoyancy pressure differential across the fault through time, attributed to increasing sealing properties as compaction affects the fault during progressive burial. Transient increases in up-fault permeability during periodic reactivation may lead to leakage of fault-bounded hydrocarbon traps, as has been found for several cases in the northern North Sea for example (Wiprut and Zoback, 2002). On production time scales, faults which initially sealed significant hydrocarbon-related pressure differences may become leaking as one compartment is depleted (e.g. Dincau, 1998) and stress changes related to depletion may render the fault unstable in certain cases, leading to up-fault leakage during slip (Cuisiat et al, 2010).

One exception to the general paucity of direct industry measurements of fault permeability is the Pathfinder well on Eugene Island, Gulf of Mexico, which shows an active normal growth fault in an overpressured siliclastic setting to have a relatively high up-fault permeability of $\sim$1 mD which sharply increases to around 1D as fluid pressure is further increased towards the minimum effective principal stress (Losh and Haney, 2006). A similar observation was made from data from an ODP borehole through the basal thrust of the Barbados accretionary prism (Screaton et al., 1990). Seismic data shot on Eugene Island at two different times over a seven year interval image the same overpressure pulse in two different places – around 1 km apart, leading to large-scale permeability estimates of around 0.1 Darcy and the suggestion that faults can "burp" such overpressure pulses upwards (Haney et al., 2005).

Healing of macro and microfracture networks in damaged rocks, in the same way as for healing of fault gouge, is an important temporal process in fault zones. The lifetime of fracture networks is needed to predict cyclic fault zone permeability at depth. Seismological evidence has shown that the recovery of P and S wave velocities (presumably related to healing of fracture damage) following the 1992 Landers earthquake is quite rapid (<10 years) (Vidale and Li, 2003). This recovery may only partially heal fault fracture damage as the low-velocity zone surrounding faults appears to be long-lived (Cochran et al., 2009).

5. Concluding remarks

Recent advances in the study of the structure, mechanics and fluid flow properties of faults and fault systems have been reviewed. The importance of the interplay of these three properties was emphasized. We conclude this work by highlighting some of the key areas of ongoing research.

In terms of fault zone structure, the heterogeneity and along fault variability are still poorly known. For example, seismological methods are necessary to determine the structure of fault zones at depth. Hence, if we are to reconcile the structure of fault zones at depth with that observed at the surface, we must better understand the dependence of seismological parameters on the physical properties of the fault rocks. Basin-scale fault systems can benefit from revised models of fault growth related to geometric and kinematic coherence. The impact of new 3D seismic datasets has the potential to greatly enhance our understanding of fault growth by providing a detailed view of growth strata that are intimately associated with the growth of faults and development of fault systems.

Our understanding of the mechanics of faulting and earthquakes is still limited. The currently unresolved question of weak faulting has helped to focus efforts, but direct observation via fault-drilling projects is necessary to resolve 2010. Even then, the drill hole has to penetrate a "representative" portion of the fault zone, with all the inherent problems of fault-zone heterogeneity previously mentioned. We can improve our knowledge of the mechanics of earthquakes by integrating data from seismology, experiments and field geology. A key aspect is to improve our understanding of the manifestations of seismic slip and its thermal effects in natural fault rocks, if this is possible. This may be aided in the future with comparison with microstructures developed in high velocity experiments. Experiments (at both high and low velocity) must aim to understand the underlying physics of slip.

Fluid flow around faults is dictated by 3D fault zone structure and, as previously mentioned, this is likely to be heterogeneous. Investigations of along-fault flow, in particular within crystalline rocks at depth, show that flow can be dominated by a small number of fractures within the surrounding damage zone. Recent efforts have helped to characterize the damage surrounding faults and we can potentially reconcile this with laboratory measurements of various fault-zone components (e.g. fault core or damage zone). However, there remains a pressing need for a greater number of in situ measurements over large areas, such as those exposed within tunnels that characterize both the permeability of individual features and whole fault zones at depth. Our understanding of the temporal evolution of fault-zone permeability is still limited, but we can address this by a combination of field and laboratory measurements.

Overall, as many aspects of faulting and fault systems are highly interrelated, an integrated approach is necessary to make progress in understanding their structure, mechanics and fluid flow properties. This integrated approach will necessarily involve many different disciplines, from field geology, laboratory measurements, geophysical measurements, modelling (numerical and experimental), and direct observation of faults through drilling.

Acknowledgements

DRF thanks the Departamento de Geologia, Universidad de Chile for their hospitality during the preparation of this manuscript. We thank Bob Holdsworth for providing a thorough review that improved the manuscript.

References

Aharonov, E., Tenthorey, E., Scholz, C.H., 1998. Precipitation sealing and diagenesis – 2. Theoretical analysis. Journal of Geophysical Research – Solid Earth 103 (B10), 23969–23981.
Allan, U.S., 1989. Model for hydrocarbon migration and entrapment within faulted structures. American Association of Petroleum Geologists Bulletin 73, 803–811.
Ampuero, J.P., Rubin, A.M., 2008. Earthquake nucleation on rate and state faults - aging and slip laws. Journal of Geophysical Research – Solid Earth 113 (B1).
Anastasio, D.J., Erslev, E.A., Fisher, D.M., 1997. Preface: fault-related folding. Journal of Structural Geology 19, v–vi.
Anders, M.H., Wiltschko, D.V., 1994. Microfracturing, paleostress and the growth of faults. Journal of Structural Geology 16 (6), 795–815.
Axen, G.J., 2007. Research focus: significance of large-displacement, low-angle normal faults. Geology 35 (3), 287–288.
Balsamo, F., Storti, F., Salvini, F., Silva, A., Lima, C., 2010. Structural and petrophysical evolution of extensional fault zones in low-porosity, poorly lithified sandstones of the Barreiras Formation, NE Brazil. Journal of Structural Geology 32 (11), 1806–1826.
Baudon, C., Cartwright, J., 2008. Early stage evolution of growth faults: 3D seismic insights from the Levant Basin, Eastern Mediterranean. Journal of Structural Geology 30 (7), 888–898.
Beeler, N.M., Hickman, S.H., 2004. Stress-induced, time-dependent fracture closure at hydrothermal conditions. Journal of Geophysical Research 109.
Berg, S.S., Skar, T., 2005. Controls on damage zone asymmetry of a normal fault zone: outcrop analyses of a segment of the Moab fault, SE Utah. Journal Of Structural Geology 27 (10), 1803–1822.
Beroza, G.C., Ellsworth, W.L., 1996. Properties of the seismic nucleation phase. Tectonophysics 261 (1–3), 209–227.
Biegel, R.L., Sammis, C.G., 2004. Relating fault mechanics to fault zone structure. Advances in Geophysics 47, 65–111.
Biegel, R.L., Sammis, C.G., Rosakis, A.J., 2008. An experimental study of the effect of off-fault damage on the velocity of a slip pulse. Journal of Geophysical Research – Solid Earth 113 (B4).
Bizzarri, A., Cocco, M., 2006. A thermal pressurization model for the spontaneous dynamic rupture propagation on a three-dimensional fault: 2. Traction evolution and dynamic parameters. Journal of Geophysical Research – Solid Earth 111 (B5).
Blanpied, M.L., Lockner, D.A., Byerlee, J.D., 1992. An earthquake mechanism based on rapid sealing of faults. Nature 358 (6387), 574–576.

Blanpied, M.L., Marone, C.J., Lockner, D.A., Byerlee, J.D., King, D.P., 1998. Quantitative measure of the variation in fault rheology due to fluid–rock interactions. Journal of Geophysical Research – Solid Earth 103 (B5), 9691–9712.

Blenkinsop, T.G., 2008. Relationships between faults, extension fractures and veins, and stress. Journal of Structural Geology 30 (5), 622–632.

Bolton, A.J., Maltman, A.J., Clennell, M.B., 1998. The importance of overpressure timing and permeability evolution in fine-grained sediments undergoing shear. Journal of Structural Geology 20 (8), 1013–1022.

Boness, N.L., Zoback, M.D., 2006. A multiscale study of the mechanisms controlling shear velocity anisotropy in the San Andreas Fault Observatory at depth. Geophysics 71 (5), F131–F146.

Bonnet, E., Bour, O., Odling, N.E., Davy, P., Main, I., Cowie, P., Berkowitz, B., 2001. Scaling of fracture systems in geological media. Reviews of Geophysics 39 (3), 347–383.

Bos, B., Peach, C.J., Spiers, C.J., 2000. Frictional-viscous flow of simulated fault gouge caused by the combined effects of phyllosilicates and pressure solution. Tectonophysics 327 (3-4), 173–194.

Bos, B., Spiers, C.J., 2001. Experimental investigation into the microstructural and mechanical evolution of phyllosilicate-bearing fault rock under conditions favouring pressure solution. Journal of Structural Geology 23 (8), 1187–1202.

Bowden, F.P., Tabor, D., 1950. The Friction and Lubrication of Solids. Oxford University Press.

Bretan, P., Yielding, G., Jones, H., 2003. Using calibrated shale gouge ratio to estimate hydrocarbon column heights. AAPG Bulletin 87 (3), 397–413.

Brister, B.S., Stephens, W.C., Norman, G.A., 2002. Structure, stratigraphy, and hydrocarbon system of a Pennsylvanian pull-apart basin in north-central Texas. AAPG Bulletin 86 (1), 1–20.

Brown, S., Caprihan, A., Hardy, R., 1998. Experimental observation of fluid flow channels in a single fracture. Journal of Geophysical Research – Solid Earth 103 (B3), 5125–5132.

Brown, S.R., Bruhn, R.L., 1998. Fluid permeability of deformable fracture networks. Journal of Geophysical Research – Solid Earth 103 (B2), 2489–2500.

Brune, J.N., Henyey, T.L., Roy, R.F., 1969. Heat flow, stress, and rate of slip along the San Andreas Fault, California. Journal of Geophysical Research 74, 3821–3827.

Bull, J.M., Barnes, P.M., Lamarche, G., Sanderson, D.J., Cowie, P.A., Taylor, S.K., Dix, J.K., 2006. High-resolution record of displacement accumulation on an active normal fault: implications for models of slip accumulation during repeated earthquakes. Journal of Structural Geology 28 (7), 1146–1166.

Byerlee, J., 1978. Friction of rocks. Pageoph 116, 615–626.

Byerlee, J., 1990. Friction, overpressure and fault normal compression. Geophysical Research Letters 17 (12), 2109–2112.

Byerlee, J., 1993. Model for episodic flow of high-pressure water in fault zones before earthquakes. Geology 21 (4), 303–306.

Caine, J.S., Evans, J.P., Forster, C.B., 1996. Fault zone architecture and permeability structure. Geology 24 (11), 1025–1028.

Caine, J.S., Bruhn, R.L., Forster, C.B., 2010. Internal structure, fault rocks, and inferences regarding deformation, fluid flow, and mineralization in the seismogenic stillwater normal fault, Dixie Valley, Nevada. Journal of Structural Geology 32 (11), 1576–1589.

Cartwright, J.A., Trudgill, B.D., Mansfield, C.S., 1995. Fault growth by segment linkage - an explanation for scatter in maximum displacement and trace length data from the canyonlands grabens of SE Utah. Journal of Structural Geology 17 (9), 1319–1326.

Cembrano, J., Gonzalez, G., Arancibia, G., Ahumada, I., Olivares, V., Herrera, V., 2005. Fault zone development and strain partitioning in an extensional strike-slip duplex: A case study from the Mesozoic Atacama fault system, Northern Chile. Tectonophysics 400 (1–4), 105–125.

Chery, J., Zoback, M.D., Hickman, S., 2004. A mechanical model of the San Andreas fault and SAFOD pilot hole stress measurements. Geophysical Research Letters 31 (15).

Chester, F.M., 1994. Effects of temperature on friction: constitutive equations and experiments with quartz gouge. Journal of Geophysical Research 99 (B4), 7247–7261.

Chester, F.M., Logan, J.M., 1986. Implications for mechanical-properties of brittle faults from observations of the Punchbowl fault zone, California. Pure and Applied Geophysics 124 (1-2), 79–106.

Chester, F.M., Friedman, M., Logan, J.M., 1985. Foliated cataclasites. Tectonophysics 111 (1–2), 139–146.

Chester, F.M., Evans, J.P., Biegel, R.L., 1993. Internal structure and weakening mechanisms of the San-Andreas fault. Journal of Geophysical Research – Solid Earth 98 (B1), 771–786.

Chester, J.S., Chester, F.M., Kronenberg, A.K., 2005. Fracture surface energy of the Punchbowl fault, San Andreas system. Nature 437 (7055), 133–136.

Chiaraluce, L., Chiarabba, C., Collettini, C., Piccinini, D., Cocco, M., 2007. Architecture and mechanics of an active low-angle normal fault: Alto Tiberina Fault, northern Apennines, Italy. Journal of Geophysical Research – Solid Earth 112 (B10), B10310. doi:10.1029/2007JB005015.

Childs, C., Manzocchi, T., Walsh, J.J., Bonson, C.G., Nicol, A., Schopfer, M.P.J., 2009. A geometric model of fault zone and fault rock thickness variations. Journal of Structural Geology 31 (2), 117–127.

Christie-Blick, N., Biddle, K.T., 1985. Deformation and basin formation along strike-slip faults. Strike-slip deformation, basin formation, and sedimentation. pp. 1–34.

Cochran, E.S., Li, Y.G., Shearer, P.M., Barbot, S., Fialko, Y., Vidale, J.E., 2009. Seismic and geodetic evidence for extensive, long-lived fault damage zones. Geology 37 (4), 315–318.

Collettini, C., Holdsworth, R.E., 2004. Fault zone weakening and character of slip along low-angle normal faults: insights from the Zuccale fault, Elba, Italy. Journal of the Geological Society 161, 1039–1051.

Collettini, C., Sibson, R.H., 2001. Normal faults, normal friction? Geology 29 (10), 927–930.

Collettini, C., Niemeijer, A., Viti, C., Marone, C., 2009a. Fault zone fabric and fault weakness. Nature.

Collettini, C., Viti, C., Smith, S.A.F., Holdsworth, R.E., 2009b. Development of interconnected talc networks and weakening of continental low-angle normal faults. Geology 37 (6), 567–570.

Cook, J.E., Dunne, W.M., Onasch, C.A., 2006. Development of a dilatant damage zone along a thrust relay in a low-porosity quartz arenite. Journal of Structural Geology 28 (5), 776–792.

Cosgrove, J.W., Ameen, M.S., 2000. Forced folds and fractures. In: Geological Society of London, Special Publications, vol. 169.

Cowie, P.A., Attal, M., Tucker, G.E., Whittaker, A.C., Naylor, M., Ganas, A., Roberts, G.P., 2006. Investigating the surface process response to fault interaction and linkage using a numerical modelling approach. Basin Research 18 (3), 231–266.

Cox, S.F., Knackstedt, M.A., Braun, J., 2001. Principles of structural control on permeability and fluid flow in hydrothermal systems. Reviews in Economic Geology 14, 1–24.

Crawford, B.R., Faulkner, D.R., Rutter, E.H., 2008. Strength, porosity, and permeability development during hydrostatic and shear loading of synthetic quartz-clay fault gouge. Journal of Geophysical Research – Solid Earth 113 (B3).

Cuisiat, F., Jostad, H.P., Andresen, L., Skurtveit, E., Skomedal, E., Hettema, M., Lyslo, K., 2010. Geomechanical integrity of sealing faults during depressurization of the Statfjord field. Journal of Structural Geology 32 (11), 1754–1767.

Cristallini, E.O., Allmendinger, R.W., 2001. Pseudo 3-D modeling of trishear fault-propagation folding. Journal of Structural Geology 23 (12), 1883–1899.

d'Alessio, M., Martel, S.J., 2005. Development of strike-slip faults from dikes, Sequoia National Park, California. Journal of Structural Geology 27 (1), 35–49.

Dawers, N.H., Anders, M.H., 1995. Displacement-length scaling and fault linkage. Journal of Structural Geology 17 (5), 607.

de Joussineau, G., Aydin, A., 2007. The evolution of the damage zone with fault growth in sandstone and its multiscale characteristics. Journal of Geophysical Research 112.

De Paola, N., Collettini, C., Faulkner, D.R., Trippetta, F., 2008. Fault zone architecture and deformation processes within evaporitic rocks in the upper crust. Tectonics 27 (4).

Di Toro, G., Pennacchioni, G., 2005. Fault plane processes and mesoscopic structure of a strong-type seismogenic fault in tonalites (Adamello batholith, Southern Alps). Tectonophysics 402 (1–4), 55–80.

Di Toro, G., Nielsen, S., Pennacchioni, G., 2005. Earthquake rupture dynamics frozen in exhumed ancient faults. Nature 436, 1009–1012.

Di Toro, G., Hirose, T., Nielsen, S., Pennacchioni, G., Shimamoto, T., 2006. Natural and experimental evidence of melt lubrication of faults during earthquakes. Science 311 (5761), 647–649.

Dieterich, J.H., Kilgore, B., 1996. Implications of fault constitutive properties for earthquake prediction. Proceedings of the National Academy of Sciences of the United States of America 93 (9), 3787–3794.

Dieterich, J.H., Kilgore, B.D., 1994. Direct observation of frictional contacts - new insights for state-dependent properties. Pure and Applied Geophysics 143 (1–3), 283–302.

Dincau, A.R., 1998. Prediction and timing of production induced fault seal breakdown in the South Marsh Island 66 gas field. Gulf Coast Association of Geological Societies Transactions XLVIII, 21–32.

Do Nascimento, A.F., Lunn, R.J., Cowie, P.A., 2005. Modeling the heterogeneous hydraulic properties of faults using constraints from reservoir-induced seismicity. Journal of Geophysical Research – Solid Earth 110 (B9).

Dockrill, B., Shipton, Z.K., 2010. Structural controls on leakage from a natural CO_2 geologic storage site: central Utah. U.S.A. Journal of Structural Geology 32 (11), 1768–1782.

Dor, O., Ben-Zion, Y., Rockwell, T.K., Brune, J., 2006. Pulverized rocks in the Mojave section of the San Andreas Fault Zone. Earth and Planetary Science Letters 245 (3–4), 642–654.

Douglas, M., Clark, I.D., Raven, K., Bottomley, D., 2000. Groundwater mixing dynamics at a Canadian Shield mine. Journal of Hydrology 235 (1–2), 88–103.

Eichhubl, P., D'Onfro, P.S., Aydin, A., Waters, A., McCarty, D.K., 2005. Structure, petrophysics, and diagenesis of shale entrained along a normal fault at Black Diamond Mines, California – implications for fault seal. AAPG Bulletin 89 (9), 1113–1137.

Eichhubl, P., Davatzes, N.C., Becker, S.P., 2009. Structural and diagenetic control of fluid migration and cementation along the Moab fault, Utah. AAPG Bulletin 93 (5), 653–681.

Ellsworth, W.L., Beroza, G.C., 1995. Seismic evidence for a earthquake nucleation phase. Science 268 (5212), 851–855.

Escartin, J., Andreani, M., Hirth, G., Evans, B., 2008. Relationships between the microstructural evolution and the rheology of talc at elevated pressures and temperatures. Earth and Planetary Science Letters 268 (3–4), 463–475.

Evans, J.P., 1990. Thickness displacement relationships for fault zones. Journal of Structural Geology 12 (8), 1061–1065.

Evans, J.P., Chester, F.M., 1995. Fluid–rock interaction in faults of the San-Andreas system – inferences from San-Gabriel fault rock geochemistry and microstructures. Journal of Geophysical Research – Solid Earth 100 (B7), 13007–13020.

Evans, K.F., Genter, A., Sausse, J., 2005. Permeability creation and damage due to massive fluid injections into granite at 3.5 km at Soultz: 1. Borehole observations. Journal of Geophysical Research – Solid Earth 110 (B4).
Fairley, J.P., 2009. Modeling fluid flow in a heterogeneous, fault-controlled hydrothermal system. Geofluids 9 (2), 153–166.
Fairley, J.P., Hinds, J.J., 2004. Field observation of fluid circulation patterns in a normal fault system. Geophysical Research Letters 31, 1–4.
Faulkner, D.R., 2004. A model for the variation in permeability of clay-bearing fault gouge with depth in the brittle crust. Geophysical Research Letters 31 (19), 5.
Faulkner, D.R., Lewis, A.C., Rutter, E.H., 2003. On the internal structure and mechanics of large strike-slip fault zones: field observations of the Carboneras fault in southeastem Spain. Tectonophysics 367 (3–4), 235–251.
Faulkner, D.R., Mitchell, T.M., Healy, D., Heap, M.J., 2006. Slip on 'weak' faults by the rotation of regional stress in the fracture damage zone. Nature 444 (7121), 922–925.
Faulkner, D.R., Mitchell, T.M., Rutter, E.H., Cembrano, J., 2008. On the structure and mechanical properties of large strike-slip faults. In: Wibberley, C.A.J., Kurz, W., Imber, J., Holdsworth., R.E., Collettini, C. (Eds.), Structure of Fault Zones: Implications for Mechanical and Fluid-flow Properties. Geological Society of London Special Publication, vol. 299, pp. 139–150.
Faulkner, D.R., Rutter, E.H., 1998. The gas permeability of clay-bearing fault gouge at 20°C. In: Jones, G., Fisher, Q., Knipe, R.J. (Eds.), Faults, Fault Sealing and Fluid Flow in Hydrocarbon Reservoirs. Geological Society of London, Special Publication, vol. 147, pp. 147–156.
Faulkner, D.R., Rutter, E.H., 2000. Comparisons of water and argon permeability in natural clay-bearing fault gouge under high pressure at 20 degrees C. Journal of Geophysical Research – Solid Earth 105 (B7), 16415–16426.
Faulkner, D.R., Rutter, E.H., 2001. Can the maintenance of overpressured fluids in large strike-slip fault zones explain their apparent weakness? Geology 29 (6), 503–506.
Faulkner, D.R., Rutter, E.H., 2003. The effect of temperature, the nature of the pore fluid, and subyield differential stress on the permeability of phyllosilicate-rich fault gouge. Journal of Geophysical Research – Solid Earth 108 (B5).
Ferrill, D.A., Winterle, J., Wittmeyer, G., Sims, D., Colton, S., Armstrong, A., Morris, A.P., 1999. Stressed rock strains groundwater at Yucca Mountain, Nevada. GSA Today 9, 1–8.
Fossen, H., Schultz, R.A., Shipton, Z.K., Mair, K., 2007. Deformation bands in sandstone: a review. Journal of the Geological Society 164, 755–769.
Freeman, B., Boult, P., Yielding, G., Menpez, S., 2010. Using empirical geological rules to reduce structural uncertainty in seismic interpretation of faults. Journal of Structural Geology 32 (11), 1668–1676.
Frye, K.M., Marone, C., 2002. Effect of humidity on granular friction at room temperature. Journal of Geophysical Research – Solid Earth 107 (B11).
Gawthorpe, R.L., Sharp, I., Underhill, J.R., Gupta, S., 1997. Linked sequence stratigraphic and structural evolution of propagating normal faults. Geology 25 (9), 795–798.
Giger, S.B., Tenthorey, E., Cox, S.F., Gerald, J.D.F., 2007. Permeability evolution in quartz fault gouges under hydrothermal conditions. Journal of Geophysical Research – Solid Earth 112 (B7).
Goldsby, D.L., Tullis, T.E., 2002. Low frictional strength of quartz rocks at subseismic slip rates. Geophysical Research Letters 29.
Gratier, J.P., Guiguet, R., Renard, F., Jenatton, L., Bernard, D., 2009. A pressure solution creep law for quartz from indentation experiments. Journal of Geophysical Research – Solid Earth 114.
Gratier, J.P., Renard, F., Labaume, P., 1999. How pressure solution creep and fracturing processes interact in the upper crust to make it behave in both a brittle and viscous manner. Journal of Structural Geology 21 (8–9), 1189–1197.
Grauls, D., Pascaud, F., Rives, T., 2002. Quantitative fault seal assessment in hydrocarbon-compartmentalised structures using fluid pressure data. In: Koestler, A.G., Hunsdale, R. (Eds.), Hydrocarbon Seal Quantification. NPF Special Publication, vol. 11, pp. 141–156.
Green, H.W., Marone, C., 2002. Instability of deformation. Reviews in Mineralogy and Geochemistry 51, 181–199.
Gueydan, F., Leroy, Y.M., Jolivet, L., Agard, P., 2003. Analysis of continental midcrustal strain localization induced by microfracturing and reaction-softening. Journal of Geophysical Research – Solid Earth 108 (B2).
Haines, S.H., van der Pluijm, B.A., Ikari, M.J., Saffer, D.M., Marone, C., 2009. Clay fabric intensity in natural and artificial fault gouges: implications for brittle fault zone processes and sedimentary basin clay fabric evolution. Journal of Geophysical Research – Solid Earth 114.
Han, R., Shimamoto, T., Hirose, T., Ree, J.H., Ando, J., 2007. Ultralow friction of carbonate faults caused by thermal decomposition. Science 316 (5826), 878–881.
Harding, T.P., 1990. Identification of wrench faults using subsurface structural data: criteria and pitfalls. American Association of Petroleum Geologists Bulletin 74 (10), 1590–1609.
Haney, M.M., Snieder, R., Sheiman, J., Losh, S., 2005. A moving fluid pulse in a fault zone. Nature 437, 46.
Henza, A.A., Withjack, M.O., Schlische, R.W., 2010. Normal-fault development during two phases of non-coaxial extension: An experimental study. Journal of Structural Geology 32 (11), 1656–1667.
Heaton, T.H., 1990. Evidence for and implications of self-healing pulses of slip in earthquake rupture. Physics of the Earth and Planetary Interiors 64 (1), 1–20.
Hickman, S., Zoback, M., 2004. Stress orientations and magnitudes in the SAFOD pilot hole. Geophysical Research Letters 31 (15).
Hickman, S.H., Evans, B., 1995. Kinetics of pressure solution at halite-silica interfaces and intergranular clay films. Journal of Geophysical Research – Solid Earth 100 (B7), 13113–13132.
Hickman, S., Sibson, R., Bruhn, R., 1995. Introduction to special section – mechanical involvement of fluids in faulting. Journal of Geophysical Research – Solid Earth 100 (B7), 12831–12840.
Hirose, T., Bystricky, M., 2007. Extreme dynamic weakening of faults during dehydration by coseismic shear heating. Geophysical Research Letters 34 (14).
Holdsworth, R.E., 2004. Weak faults – rotten cores. Science 303 (5655), 181–182.
Holyoke, C.W., Tullis, J., 2006. The interaction between reaction and deformation: an experimental study using a biotite plus plagioclase plus quartz gneiss. Journal of Metamorphic Geology 24 (8), 743–762.
Hubbert, M.K., Rubey, W.W., 1959. Role of fluid pressure in mechanics of overthrust faulting 1. Mechanics of fluid filled porous solids and its application of overthrust faulting. Geological Society of America Bulletin 70 (2), 115–166.
Ikari, M.J., Saffer, D.M., Marone, C., 2009. Frictional and hydrologic properties of clay-rich fault gouge. Journal of Geophysical Research 114.
Imber, J., Holdsworth, R.E., Butler, C.A., Strachan, R.A., 2001. A reappraisal of the Sibson-Scholz fault zone model: the nature of the frictional to viscous ("brittle–ductile") transition along a long-lived, crustal-scale fault, Outer Hebrides, Scotland. Tectonics 20 (5), 601–624.
Ishii, E., Funaki, H., Tokiwa, T., Ota, K. Relationship between growth mechanism of faults and permeability variations with depth in siliceous mudstone. Journal of Structural Geology, in press.
Janecke, S.U., Vandenburg, C.J., Blankenau, J.J., 1998. Geometry, mechanisms and significance of extensional folds from examples in the Rocky Mountain Basin and Range province, USA. Journal of Structural Geology 20 (7), 841–856.
Janssen, C., Wagner, F.C., Zang, A., Dresen, G., 2001. Fracture process zone in granite: a microstructural analysis. International Journal of Earth Sciences 90 (1), 46–59.
Jefferies, S.P., Holdsworth, R.E., Shimamoto, T., Takagi, H., Lloyd, G.E., Spiers, C.J., 2006a. Origin and mechanical significance of foliated cataclastic rocks in the cores of crustal-scale faults: examples from the Median Tectonic Line, Japan. Journal of Geophysical Research – Solid Earth 111 (B12).
Jefferies, S.P., Holdsworth, R.E., Wibberley, C.A.J., Shimamoto, T., Spiers, C.J., Niemeijer, A.R., Lloyd, G.E., 2006b. The nature and importance of phyllonite development in crustal-scale fault cores: an example from the Median Tectonic Line, Japan. Journal of Structural Geology 28 (2), 220–235.
Johansen, T.E.S., Fossen, H., Kluge, R., 2005. The impact of syn-faulting porosity reduction on damage zone architecture in porous sandstone: an outcrop example from the Moab Fault, Utah. Journal of Structural Geology 27 (8), 1469–1485.
Jourde, H., Flodin, E.A., Aydin, A., Durlofsky, L.J., Wen, X.H., 2002. Computing permeability of fault zones in eolian sandstone from outcrop measurements. AAPG Bulletin 86 (7), 1187–1200.
Kanamori, H., Brodsky, E.E., 2004. The physics of earthquakes. Reports on Progress in Physics 67 (8). doi:10.1088/0034-4885/67/8/R03 pii: S0034-4885(04)25227-7.
Kanamori, H., Rivera, L., 2006. Energy partitioning during an earthquake. In: Abercrombie, R., McGarr, A., Kanamori, H., Di Toro, G. (Eds.), Earthquakes: Radiated Energy and the Physics of Faulting. Geophysical Monograph Series, vol. 170, pp. 3–15.
Karner, S.L., Marone, C., Evans, B., 1997. Laboratory study of fault healing and lithification in simulated fault gouge under hydrothermal conditions. Tectonophysics 277 (1–3), 41–55.
Kim, Y.S., Peacock, D.C.P., Sanderson, D.J., 2004. Fault damage zones. Journal of Structural Geology 26 (3), 503–517.
Kim, Y.S., Sanderson, D.J., 2005. The relationship between displacement and length of faults: a review. Earth-Science Reviews 68 (3–4), 317–334.
Kirkpatrick, J.D., Shipton, Z.K., Evans, J.P., Micklethwaite, S., Lim, S.J., McKillop, P., 2008. Strike-slip fault terminations at seismogenic depths: the structure and kinematics of the Glacier Lakes fault, Sierra Nevada United States. Journal of Geophysical Research – Solid Earth 113 (B4).
Kohlstedt, D.L., Evans, B., Mackwell, S.J., 1995. Strength of the lithosphere - constaints imposed by laboratory experiments. Journal of Geophysical Research – Solid Earth 100 (B9), 17587–17602.
Kristensen, M.B., Childs, C.J., Korstgard, J.A., 2008. The 3D geometry of small-scale relay zones between normal faults in soft sediments. Journal of Structural Geology 30 (2), 257–272.
Lachenbruch, A.H., Sass, J.H., 1980. Heat-flow and energetics of the San-Andreas fault zone. Journal of Geophysical Research 85 (Nb11), 6185–6222.
Lindsay, N.G., Murphy, F.C., Walsh, J.J., Watterson, J., 1993. Outcrop studies of shale smear on fault surfaces. In: International Association of Sedimentology, Special Publications, vol. 15 113–123.
Logan, J.M., Friedman, M., Higgs, N.G., Dengo, C.A. and Shimamoto, T. 1979. Experimental studies of simulated gouge and their application to studies of natural fault zones. Analysis of actual fault zones in bedrock. U.S. Geological Survey Open File Report 79-1239, pp. 305–343.
Logan, J.M., Rauenzahn, K.A., 1987. Frictional dependence of gouge mixtures of quartz and montmorillonite on velocity, composition and fabric. Tectonophysics 144 (1–3), 87–108.
Lohr, T., Krawczyk, C.M., Oncken, O., Tanner, D.C., 2008. Evolution of a fault surface from 3D attribute analysis and displacement measurements. Journal of Structural Geology 30 (6), 690–700.
Losh, S., Haney, M., 2006. Episodic fluid flow in an aseismic overpressured growth fault, northern Gulf of Mexico. In: Abercrombie, R., McGarr, A., Di Toro, G., Kanamori, H. (Eds.), Earthquakes: Radiated Energy and the Physics of Faulting.

American Geophysical Union Geophysical Monograph Series, vol. 170, pp. 199–206.
Lunn, R.J., Willson, J.P., Shipton, Z.K., Moir, H., 2008. Simulating brittle fault growth from linkage of preexisting structures. Journal of Geophysical Research – Solid Earth 113 (B7).
Main, I.G., Kwon, O., Ngwenya, B.T., Elphick, S.C., 2000. Fault sealing during deformation-band growth in porous sandstone. Geology 28 (12), 1131–1134.
Manzocchi, T., Walsh, J.J., Nell, P., Yielding, G., 1999. Fault transmissibility multipliers for flow simulation models. Petroleum Geoscience 5 (1), 53–63.
Mares, V.M., Kronenberg, A.K., 1993. Experimental deformation of muscovite. Journal of Structural Geology 15 (9–10), 1061–1075.
Mariani, E., Brodie, K.H., Rutter, E.H., 2006. Experimental deformation of muscovite shear zones at high temperatures under hydrothermal conditions and the strength of phyllosilicate-bearing faults in nature. Journal of Structural Geology 28 (9), 1569–1587.
Marone, C., 1998. Laboratory-derived friction laws and their application to seismic faulting. Annual Review of Earth and Planetary Sciences 26, 643–696.
Marone, C., Kilgore, B., 1993. Scaling of the critical slip distance for seismic faulting with shear strain in fault zones. Nature 362 (6421), 618–621.
Marone, C., Richardson, E., 2006. Do earthquakes rupture piece by piece or all together? Science 313 (5794), 1748–1749.
Marone, C., Scholz, C.H., 1989. Particle-size distribution and microstructures within simulated fault Gouge. Journal of Structural Geology 11 (7), 799–814.
Martel, S.J., Pollard, D.D., Segall, P., 1988. Development of simple strike-slip fault zones, Mount Abbot Quadrangle, Sierra Nevada, California. Geological Society of America Bulletin 100 (9), 1451–1465.
Matthai, S.K., Belayneh, M., 2004. Fluid flow partitioning between fractures and a permeable rock matrix. Geophysical Research Letters 31 (7).
McClay, K.R., 2004. Thrust tectonics and hydrocarbon systems. AAPG Memoir 82, 667.
McGrath, A.G., Davison, I., 1995. Damage zone geometry around fault tips. Journal of Structural Geology 17 (7), 1011–1024.
Medeiros W.E., do Nascimento, A.F., Alves da Silva, F.C., Destro, N., Demétrio, J.G.A. Evidence of hydraulic connectivity across deformation bands from field pumping tests: Two examples from Tucano Basin, NE Brazil. Journal of Structural Geology, this issue.
Micarelli, L., Benedicto, A., Wibberley, C.A.J., 2006. Structural evolution and permeability of normal fault zones in highly porous carbonate rocks. Journal of Structural Geology 28 (7), 1214–1227.
Miller, S.A., Collettini, C., Chiaraluce, L., Cocco, M., Barchi, M., Kaus, B.J.P., 2004. Aftershocks driven by a high-pressure CO_2 source at depth. Nature 427 (6976), 724–727.
Mitchell, T.M., Faulkner, D.R., 2008. Experimental measurements of permeability evolution during triaxial compression of initially intact crystalline rocks and implications for fluid flow in fault zones. Journal of Geophysical Research – Solid Earth 113 (B11).
Mitchell, T.M., Faulkner, D.R., 2009. The nature and origin of off-fault damage surrounding strike-slip fault zones with a wide range of displacements: A field study from the Atacama fault zone, northern Chile. Journal of Structural Geology 31, 802–816.
Mizoguchi, K., Hirose, T., Shimamoto, T., Fukuyama, E., 2008. Internal structure and permeability of the Nojima fault, southwest Japan. Journal of Structural Geology 30 (4), 513–524.
Mo, Y.F., Turner, K.T., Szlufarska, I., 2009. Friction laws at the nanoscale. Nature 457 (7233), 1116–1119.
Moir, H., Lunn, R., Shipton, Z., Kirkpatrick, J. Simulating brittle fault evolution from networks of pre-existing structures. Journal of Structural Geology, this issue.
Moore, D.E., Lockner, D.A., 2004. Crystallographic controls on the frictional behavior of dry and water-saturated sheet structure minerals. Journal of Geophysical Research – Solid Earth 109 (B3).
Moore, D.E., Lockner, D.A., 2008. Talc friction in the temperature range 25 degrees-400 degrees C: relevance for fault-zone weakening. Tectonophysics 449 (1–4), 120–132.
Moore, D.E., Lockner, D.A., Tanaka, H., Iwata, K., 2004. The coefficient of friction of Chrysotile gouge at seismogenic depths. International Geology Review 46 (5), 385–398.
Moore, D.E., Rymer, M.J., 2007. Talc-bearing serpentinite and the creeping section of the San Andreas fault. Nature 448 (7155), 795–797.
Morrow, C.A., Lockner, D.A., 1994. Permeability differences between surface-derived and deep drillhole core samples. Geophysical Research Letters 21 (19), 2151–2154.
Morrow, C.A., Moore, D.E., Lockner, D.A., 2001. Permeability reduction in granite under hydrothermal conditions. Journal of Geophysical Research – Solid Earth 106 (B12), 30551–30560.
Morrow, C.A., Radney, B., Byerlee, J.D., 1992. Frictional strength and the effective pressure law of montmorillonite and illite clays. In: Evans, B., Wong, T.-F. (Eds.), Fault Mechanics and Transport Properties of Rocks. Academic Press, pp. 69–88.
Nakatani, M., 2001. Conceptual and physical clarification of rate and state friction: frictional sliding as a thermally activated rheology. Journal of Geophysical Research – Solid Earth 106 (B7), 13347–13380.
Nakatani, M., Scholz, C.H., 2004a. Frictional healing of quartz gouge under hydrothermal conditions: 1. Experimental evidence for solution transfer healing mechanism. Journal of Geophysical Research – Solid Earth 109 (B7).
Nakatani, M., Scholz, C.H., 2004b. Frictional healing of quartz gouge under hydrothermal conditions: 2. Quantitative interpretation with a physical model. Journal of Geophysical Research – Solid Earth 109 (B7).
Nemser, E.S., Cowan, D.S., 2009. Downdip segmentation of strike-slip fault zones in the brittle crust. Geology 37 (5), 419–422.
Noda, H., 2008. Frictional constitutive law at intermediate slip rates accounting for flash heating and thermally activated slip process. Journal of Geophysical Research – Solid Earth 113 (B9).
Noda, H., Dunham, E.M., Rice, J.R., 2009. Earthquake ruptures with thermal weakening and the operation of major faults at low overall stress levels. Journal of Geophysical Research 114.
Noir, J., Jacques, E., Bekri, S., Adler, P.M., Tapponnier, P., King, G.C.P., 1997. Fluid flow triggered migration of events in the 1989 Dobi earthquake sequence of Central Afar. Geophysical Research Letters 24 (18), 2335–2338.
Numelin, T., Marone, C., Kirby, E., 2007. Frictional properties of natural fault gouge from a low-angle normal fault, Panamint Valley, California. Tectonics 26 (2).
O'Hara, K., 2007. Reaction weakening and emplacement of crystalline thrusts: diffusion control on reaction rate and strain rate. Journal of Structural Geology 29 (8), 1301–1314.
Oda, M., Takemura, T., Aoki, T., 2002. Damage growth and permeability change in triaxial compression tests of Inada granite. Mechanics of Materials 34 (6), 313–331.
Odling, N.E., Harris, S.D., Knipe, R., 2004. Permeability scaling properties of fault damage zones in siliclastic rocks. Journal of Structural Geology 26 (9), 1727–1747.
Olsen, M.P., Scholz, C.H., Leger, A., 1998. Healing and sealing of a simulated fault gouge under hydrothermal conditions: implications for fault healing. Journal of Geophysical Research – Solid Earth 103 (B4), 7421–7430.
Peacock, D.C.P., Sanderson, D.J., 1991. Displacements, segment linkage and relay ramps in normal fault zones. Journal of Structural Geology 13 (6), 721.
Price, R.A., 1988. The mechanical paradox of large overthrusts. Geological Society of America Bulletin 100 (12), 1898–1908.
Rawling, G.C., Goodwin, L.B., Wilson, J.L., 2001. Internal architecture, permeability structure, and hydrologic significance of contrasting fault-zone types. Geology 29 (1), 43–46.
Reches, Z., Dewers, T.A., 2005. Gouge formation by dynamic pulverization during earthquake rupture. Earth and Planetary Science Letters 235 (1–2), 361–374.
Reches, Z., Lockner, D.A., 1994. Nucleation and growth of faults in brittle rocks. Journal of Geophysical Research 99 (B9), 18159–18173.
Reinen, L.A., 2000. Slip styles in a spring-slider model with a laboratory-derived constitutive law for serpentinite. Geophysical Research Letters 27 (14), 2037–2040.
Rempel, A.W., Rice, J.R., 2006. Thermal pressurization and onset of melting in fault zones. Journal of Geophysical Research – Solid Earth 111 (B9).
Renard, F., Gratier, J.P., Jamtveit, B., 2000. Kinetics of crack-sealing, intergranular pressure solution, and compaction around active faults. Journal of Structural Geology 22 (10), 1395–1407.
Revil, A., Grauls, D., Brevart, O., 2002. Mechanical compaction of sand/clay mixtures. Journal of Geophysical Research – Solid Earth 107 (B11).
Rice, J.R., 1992. Fault stress states, pore pressure distributions, and the weakness of the San Andreas fault. In: Evans, B., Wong, T.-F. (Eds.), Fault Mechanics and Transport Properties in Rocks. Academic Press, p. 28.
Rice, J.R., 2006. Heating and weakening of faults during earthquake slip. Journal of Geophysical Research – Solid Earth 111 (B5).
Rice, J.R., Lapusta, N., Ranjith, K., 2001. Rate and state dependent friction and the stability of sliding between elastically deformable solids. Journal of the Mechanics and Physics of Solids 49 (9), 1865–1898.
Roberts, G.P., Houghton, S.L., Underwood, C., Papanikolaou, I., Cowie, P.A., van Calsteren, P., Wigley, T., Cooper, F.J., McArthur, J.M., 2009. Localization of Quaternary slip rates in an active rift in 10(5) years: an example from central Greece constrained by U-234–Th-230 coral dates from uplifted paleoshorelines. Journal of Geophysical Research – Solid Earth 114.
Rowland, J.V., Sibson, R.H., 2004. Structural controls on hydrothermal flow in a segmented rift system, Taupo Volcanic Zone, New Zealand. Geofluids 4 (4), 259–283.
Rudnicki, J.W., Rice, J.R., 2006. Effective normal stress alteration due to pore pressure changes induced by dynamic slip propagation on a plane between dissimilar materials. Journal of Geophysical Research – Solid Earth 111 (B10).
Rutter, E.H., Brodie, K.H., 1995. Mechanistic interactions between deformation and metamorphism. Geological Journal 30 (3–4), 227–240.
Rutter, E.H., Maddock, R.H., Hall, S.H., White, S.H., 1986. Comparative microstructures of natural and experimentally produced clay-bearing fault gouges. Pure and Applied Geophysics 124 (1–2), 3–30.
Rutter, E.H., Mainprice, D.H., 1979. On the possibility of slow fault slip controlled by a diffusive mass transfer process. Gerlands Beitrage zur Geophysik 88, 154–162.
Saffer, D.M., Frye, K.M., Marone, C., Mair, K., 2001. Laboratory results indicating complex and potentially unstable frictional behavior of smectite clay. Geophysical Research Letters 28 (12), 2297–2300.
Saffer, D.M., Marone, C., 2003. Comparison of smectite- and illite-rich gouge frictional properties: application to the updip limit of the seismogenic zone along subduction megathrusts. Earth and Planetary Science Letters 215 (1-2), 219–235.
Saillet, E., Wibberley, C. Evolution of cataclastic faulting in high porosity sandstone, Bassin du Sud-Est, Provence, France. Journal of Structural Geology, this issue.
Sammis, C., King, G., Biegel, R., 1987. The kinematics of gouge deformation. Pure and Applied Geophysics 125 (5), 777–812.
Sammis, C.G., Ben-Zion, Y., 2008. Mechanics of grain-size reduction in fault zones. Journal of Geophysical Research – Solid Earth 113 (B2).
Savage, H.M., Brodsky, E.E. Collateral damage: capturing slip delocalization in fracture profiles. Journal of Geophysical Research, submitted for publication.

Savage, H.M., Cooke, M.L., 2010. Unlocking the effects of friction on fault damage zone models. Journal of Structural Geology 32 (11), 1732–1741.
Schlische, R.W., 1995. Geometry and origin of fault-related folds in extensional settings. AAPG Bulletin – American Association of Petroleum Geologists 79 (11), 1661–1678.
Schlische, R.W., Withjack, M.O., Eisenstadt, G., 2002. An experimental study of the secondary deformation produced by oblique-slip normal faulting. American Association of Petroleum Geologists Bulletin 86 (5), 885–906.
Schmatz, J., Vrolijk, P., Urai, J., 2010. Clay smear in normal faults - the effect of multilayers and clay cementation in water-saturated model experiments. Journal of Structural Geology 32 (11), 1834–1849.
Scholz, C.H., 1987. Wear and Gouge formation in brittle faulting. Geology 15 (6), 493–495.
Scholz, C.H., 1988. The critical slip distance for seismic faulting. Nature 336 (6201), 761–763.
Scholz, C.H., 1998. Earthquakes and friction laws. Nature 391 (6662), 37–42.
Scholz, C.H., 2002. The Mechanics of Earthquakes and Faulting. Cambridge University Press, Cambridge.
Scholz, C.H., 2006. The strength of the San Andreas fault: a critical analysis. Earthquakes: Radiated Energy and the Physics of Faulting 170, 301–311.
Schulz, S.E., Evans, J.P., 2000. Mesoscopic structure of the Punchbowl Fault, Southern California and the geologic and geophysical structure of active strike-slip faults. Journal of Structural Geology 22 (7), 913–930.
Screaton, E.J., Wuthrich, D.R., Dreiss, S.J., 1990. Permeabilities, fluid pressures, and flow rates in the Barbados ridge complex. Journal of Geophysical Research – Solid Earth and Planets 95 (B6), 8997–9007.
Scruggs, V.J., Tullis, T.E., 1998. Correlation between velocity dependence of friction and strain localization in large displacement experiments on feldspar, muscovite and biotite gouge. Tectonophysics 295 (1–2), 15–40.
Segall, P., Rice, J.R., 2006. Does shear heating of pore fluid contribute to earthquake nucleation? Journal of Geophysical Research – Solid Earth 111 (B9).
Shapiro, S.A., Huenges, E., Borm, G., 1997. Estimating the crust permeability from fluid-injection-induced seismic emission at the KTB site. Geophysical Journal International 131 (2), F15–F18.
Shaw, J.H., Connors, C., Suppe, J., 2005. Seismic interpretation of contractional fault-related folds: an AAPG seismic atlas. American Association of Petroleum Geologists Studies in Geology 53, 157.
Shipton, Z.K., Cowie, P.A., 2001. Damage zone and slip-surface evolution over μm to km scales in high-porosity Navajo sandstone, Utah. Journal of Structural Geology 23 (12), 1825–1844.
Shipton, Z.K., Cowie, P.A., 2003. A conceptual model for the origin of fault damage zone structures in high-porosity sandstone. Journal of Structural Geology 25 (8), 1343–1345.
Shipton, Z.K., Evans, J.P., Robeson, K.R., Forster, C.B., Snelgrove, S., 2002. Structural heterogeneity and permeability in faulted eolian sandstone: implications for subsurface modeling of faults. AAPG Bulletin 86 (5), 863–883.
Shipton, Z.K., Evans, J.P., Thompson, L.B., 2005. The geometry and thickness of deformation band fault core, and its influence on sealing characteristics of deformation band fault zones. American Association of Petroleum Geologists Memoir 85, 181–195.
Shipton, Z.K., Soden, A.M., Kirkpatrick, J.D., Bright, A.M., Lunn, R.J., 2006. How thick is a fault? Fault displacement-thickness scaling revisited. Earthquakes: Radiated Energy and the Physics of Faulting 170, 193–198.
Sibson, R.H., 1990. Conditions for fault-valve behaviour. In: Geological Society of London, Special Publication, vol. 54 15–28.
Sibson, R.H., 2001. Seismogenic framework for hydrothermal transport and ore deposition. Reviews in Economic Geology 14, 25–50.
Sibson, R.H., 2009. Rupturing in overpressured crust during compressional inversion-the case from NE Honshu, Japan. Tectonophysics 473 (3–4), 404–416.
Sibson, R.H., Xie, G.Y., 1998. Dip range for intracontinental reverse fault ruptures: truth not stranger than friction? Bulletin of the Seismological Society of America 88 (4), 1014–1022.
Simpson, G., Gueguen, Y., Schneider, F., 2001. Permeability enhancement due to microcrack dilatancy in the damage regime. Journal of Geophysical Research – Solid Earth 106 (B3), 3999–4016.
Smith, S.A.F., Faulkner, D.R., 2010. Laboratory measurements of the frictional properties of a natural low-angle normal fault: The Zuccale fault, Elba Island, Italy. Journal of Geophysical Research 115, B02407.
Smith, S.A.F., Holdsworth, R.E., Collettini, C., Imber, J., 2007. Using footwall structures to constrain the evolution of low-angle normal faults. Journal of the Geological Society 164, 1187–1191.
Soliva, R., Benedicto, A., 2005. Geometry, scaling relations and spacing of vertically restricted normal faults. Journal of Structural Geology 27 (2), 317–325.
Soliva, R., Maertan, F., Petit, J.-P., Auzias, V. Fault static friction and fracture orientation in extensional relays; insight from field data, photoelasticity and 3D numerical modeling. Journal of Structural Geology, this issue.
Solum, J.G., van der Pluijm, B.A. Quantification of fabrics in clay gouge from the Carboneras fault, Spain and implications for fault behavior. Tectonophysics 475 (3–4), 554–562.
Sperrevik, S., Gillespie, P.A., Fisher, Q., Halvorsen, T., Knipe, R.J., 2002. Empirical estimation of fault rock properties. In: Koestler, A.G., Hunsdale, R. (Eds.), Hydrocarbon Seal Quantification. NPF Special Publications, vol. 11, pp. 109–125.
Spudich, P., Guatteri, M., 2004. The effect of bandwidth limitations on the inference of earthquake slip-weakening distance from seismograms. Bulletin of the Seismological Society of America 94 (6), 2028–2036.
Streit, J.E., Hillis, R.R., 2004. Estimating fault stability and sustainable fluid pressures for underground storage of CO_2 in porous rock. Energy 29 (9–10), 1445–1456.
Suppe, J., 1983. Geometry and kinematics of fault-bend folding. American Journal of Science 283 (7), 684–721.
Swanson, M.T., 2005. Geometry and kinematics of adhesive wear in brittle strike-slip fault zones. Journal of Structural Geology 27 (5), 871–887.
Szlufarska, I., Chandross, M., Carpick, R.W., 2008. Recent advances in single-asperity nanotribology. Journal of Physics D – Applied Physics 41 (12).
Tadokoro, K., Ando, M., Nishigami, K., 2000. Induced earthquakes accompanying the water injection experiment at the Nojima fault zone, Japan: seismicity and its migration. Journal of Geophysical Research – Solid Earth 105 (B3), 6089–6104.
Takahashi, M., Mizoguchi, K., Kitamura, K., Masuda, K., 2007. Effects of clay content on the frictional strength and fluid transport property of faults. Journal of Geophysical Research – Solid Earth 112 (B8).
Talwani, P., Cobb, J.S., Schaeffer, M.F., 1999. In situ measurements of hydraulic properties of a shear zone in northwestern South Carolina. Journal of Geophysical Research – Solid Earth 104 (B7), 14993–15003.
Talwani, P., Chen, L., Gahalaut, K., 2007. Seismogenic permeability, k(S). Journal of Geophysical Research – Solid Earth 112 (B7).
Tembe, S., Lockner, D.A., Solum, J.G., Morrow, C.A., Wong, T.F., Moore, D.E., 2006. Frictional strength of cuttings and core from SAFOD drillhole phases 1 and 2. Geophysical Research Letters 33 (23).
Tenthorey, E., Scholz, C.H., Aharonov, E., Leger, A., 1998. Precipitation sealing and diagenesis – 1. Experimental results. Journal of Geophysical Research – Solid Earth 103 (B10), 23951–23967.
Tenthorey, E., Cox, S.F., Todd, H.F., 2003. Evolution of strength recovery and permeability during fluid-rock reaction in experimental fault zones. Earth and Planetary Science Letters 206 (1–2), 161–172.
Tindall, S.E., Davis, G.H., 1999. Monocline development by oblique-slip fault-propagation folding: the East Kaibab monocline, Colorado Plateau, Utah. Journal of Structural Geology 21 (10), 1303–1320.
Tinti, E., Cocco, M., Fukuyama, E., Piatanesi, A., 2009. Dependence of slip weakening distance (D-c) on final slip during dynamic rupture of earthquakes. Geophysical Journal International 177 (3), 1205–1220.
Tinti, E., Spudich, P., Cocco, M., 2005. Earthquake fracture energy inferred from kinematic rupture models on extended faults. Journal of Geophysical Research – Solid Earth 110 (B12).
Townend, J., Zoback, M.D., 2000. How faulting keeps the crust strong. Geology 28 (5), 399–402.
Tsutsumi, A., Shimamoto, T., 1997. High-velocity frictional properties of gabbro. Geophysical Research Letters 24 (6), 699–702.
Tsutsumi, A., Nishino, S., Mizoguchi, K., Hirose, T., Uehara, S., Sato, K., Tanikawa, W., Shimamoto, T., 2004. Principal fault zone width and permeability of the active Neodani fault, Nobi fault system, Southwest Japan. Tectonophysics 379 (1–4), 93–108.
Uehara, S., Shimamoto, T., 2004. Gas permeability evolution of cataclasite and fault gouge in triaxial compression and implications for changes in fault-zone permeability structure through the earthquake cycle. Tectonophysics 378 (3–4), 183–195.
van der Zee, W., Urai, J.L., 2005. Processes of normal fault evolution in a siliciclastic sequence: a case study from Miri, Sarawak, Malaysia. Journal of Structural Geology 27 (12), 2281–2300.
Van der Zee, W., Wibberley, C.A.J., Urai, J.L., 2008. The influence of layering and pre-existing joints on the development of internal structure in normal fault zones: the Lodève basin, France. In: Wibberley, C.A.J., Kurz, W., Imber, J., Holdsworth, R.E., Collettini, C. (Eds.), The Internal Structure of Fault Zones: Implications for Mechanical and Fluid Flow Properties. Geological Society of London, Special Publication, vol. 299, pp. 57–74.
van Diggelen, E. W., De Bresser, J.H., Peach, C.J., Spiers, C.J. High shear strain behaviour of synthetic muscovite fault gouges under hydrothermal conditions. Journal of Structural Geology, this issue.
Vermilye, J.M., Scholz, C.H., 1998. The process zone: a microstructural view of fault growth. Journal of Geophysical Research – Solid Earth 103 (B6), 12223–12237.
Vidale, J.E., Li, Y.G., 2003. Damage to the shallow Landers fault from the nearby Hector Mine earthquake. Nature 421 (6922), 524–526.
Walker, J.P.F., Roberts, G.P., Cowie, P.A., Papanikolaou, I.D., Sammonds, P.R., Michetti, A.M., Phillips, R.J., 2009. Horizontal strain-rates and throw-rates across breached relay zones, central Italy: implications for the preservation of throw deficits at points of normal fault linkage. Journal of Structural Geology 31 (10), 1145–1160.
Walsh, J.J., Watterson, J., 1988. Analysis of the relationship between displacements and dimensions of faults. Journal of Structural Geology 10 (3), 239–247.
Walsh, J.J., Nicol, A., Childs, C., 2002. An alternative model for the growth of faults. Journal of Structural Geology 24 (11), 1669–1675.
Weber, K.J., Mandl, G., Pilaar, W.F., Lehner, F., Precious, R.G. 1978. The role of faults in hydrocarbon migration and trapping in Nigerian growth fault structures. In: 10th Annual Offshore Technology Conference Proceedings 4, pp. 2643–2653.
Whittaker, A.C., Attal, M., Cowie, P.A., Tucker, G.E., Roberts, G., 2008. Decoding temporal and spatial patterns of fault uplift using transient river long profiles. Geomorphology 100 (3–4), 506–526.
Wibberley, C.A.J., 2005. Initiation of basement thrust detachments by fault-zone reaction weakening. In: Bruhn, D., Burlini, L. (Eds.), High Strain Zones: Structure and Physical Properties, vol. 245. Geological Society, London, Special Publications, pp. 347–372.

Wibberley, C.A.J., McCaig, A.M., 2000. Quantifying orthoclase and albite muscovitisation sequences in fault zones. Chemical Geology 165 (3–4), 181–196.
Wibberley, C.A.J., Shimamoto, T., 2003. Internal structure and permeability of major strike-slip fault zones: the Median Tectonic Line in Mie Prefecture, Southwest Japan. Journal of Structural Geology 25 (1), 59–78.
Wibberley, C.A.J., Shimamoto, T., 2005. Earthquake slip weakening and asperities explained by thermal pressurization. Nature 436 (7051), 689–692.
Wibberley, C.A.J., Yielding, G., Di Toro, G., 2008. Recent advances in the understanding of fault zone internal structure; a review. In: Wibberley, C.A.J., Kurz, W., Imber, J., Holdsworth, R.E., Collettini, C. (Eds.), Structure of Fault Zones: Implications for Mechanical and Fluid-flow Properties. Geological Society of London Special Publication, vol. 299, pp. 5–33.
Wilkerson, M.S., Fischer, M.P., Apotria, T., 2002. Fault-related folds: the transition from 2-D to 3-D – preface. Journal of Structural Geology 24 (4), 591–592.
Wilkins, S.J., Gross, M.R., 2002. Normal fault growth in layered rocks at Split Mountain, Utah: influence of mechanical stratigraphy on dip linkage, fault restriction and fault scaling. Journal of Structural Geology 24 (9), 1413–1429.
Wilkins, S.J., Gross, M.R., Wacker, M., Eyal, Y., Engelder, T., 2001. Faulted joints: kinematics, displacement-length scaling relations and criteria for their identification. Journal of Structural Geology 23 (2–3), 315–327.
Wilson, J.E., Chester, J.S., Chester, F.M., 2003. Microfracture analysis of fault growth and wear processes, Punchbowl Fault, San Andreas System, California. Journal of Structural Geology 25 (11), 1855–1873.
Wintsch, R.P., Christoffersen, R., Kronenberg, A.K., 1995. Fluid-rock reaction weakening of fault zones. Journal of Geophysical Research – Solid Earth 100 (B7), 13021–13032.
Wiprut, D., Zoback, M., 2002. Fault reactivation, leakage potential, and hydrocarbon column heights in the northern North Sea. In: Koestler, A.G., Hunsdale, R. (Eds.), Hydrocarbon Seal Quantification. NPF Special Publication, vol. 11, pp. 203–219.
Withjack, M.O., Schlische, R.W., Olsen, P.E., 2002. Rift-basin structure and its influence on sedimentary systems. In: Society for Sedimentary Geology Special Publication, vol. 73 57–81.
Yamashita, T., Suzuki, T., 2009. Quasi-static fault slip on an interface between poroelastic media with different hydraulic diffusivity: a generation mechanism of afterslip. Journal of Geophysical Research – Solid Earth 114.
Yasuhara, H., Marone, C., Elsworth, D., 2005. Fault zone restrengthening and frictional healing: the role of pressure solution. Journal of Geophysical Research – Solid Earth 110 (B6).
Yielding, G., Freeman, B., Needham, D.T., 1997. Quantitative fault seal prediction. AAPG Bulletin – American Association of Petroleum Geologists 81 (6), 897–917.
Zhang, S.Q., Tullis, T.E., 1998. The effect of fault slip on permeability and permeability anisotropy in quartz gouge. Tectonophysics 295 (1–2), 41–52.
Zhang, S.Q., Tullis, T.E., Scruggs, V.J., 1999. Permeability anisotropy and pressure dependency of permeability in experimentally sheared gouge materials. Journal of Structural Geology 21 (7), 795–806.
Zheng, G., Rice, J.R., 1998. Conditions under which velocity-weakening friction allows a self-healing versus a cracklike mode of rupture. Bulletin of the Seismological Society of America 88 (6), 1466–1483.
Zoback, M., Hickman, S., Ellsworth, W., 2010. Scientific drilling into the San Andreas fault zone. Eos. Transactions American Geophysical Union 91 (22), 197–199.